1.D.2 *Nuclear Physics* A327 (1979) 139–171; © *North-Holland Publishing Co., Amsterdam*

QUASIPARTICLE SPECTRA NEAR THE YRAST LINE †

R. BENGTSSON ††
Nordita, Blegdamsvej 17, DK-2100 Copenhagen Ø, Denmark
and
S. FRAUENDORF
The Niels Bohr Institute, University of Copenhagen, DK-2100 Copenhagen Ø, Denmark
and
Central Institute for Nuclear Research, Rossendorf, DDR

Received 15 December 1978
(Revised 10 May 1979)

Abstract: The yrast spectra of the nuclides $68 \leq Z \leq 70$, $89 \leq N \leq 99$ are analysed in terms of quasiparticle configurations in a deformed field rotating with the frequency ω. The excitation energy, e', in the rotating frame (Routhian) and the aligned angular momentum, i, relative to the ground state band as functions of ω are extracted from the experimental rotational bands which are classified with respect to their signature, α, and parity, π. These experimental quantities are compared with the ones calculated from the quasiparticle level diagrams. Phenomena like backbending and the occurrence of aligned bands in both even-even and odd-mass nuclei and their mutual relationship are interpreted in terms of quasiparticle configurations that may cross each other with increasing frequency.

1. Introduction

Most of the experimental information about high-spin states concerns the yrast line and its vicinity, where almost all excitation energy is needed to build up the high angular momentum. The level density for such a cold rotating nucleus is relatively low. This permits employment of the concepts that have been developed for the analysis of the nuclear spectrum near the ground state. The angular momentum may be incorporated if one bases the analysis on the Routhian

$$H' = H - \omega J_x, \tag{1.1}$$

instead of the Hamiltonian H of the system. The Lagrangian multiplier ensures a finite value of the angular momentum I. The Routhian is readily recognized as the Hamiltonian in a frame of reference rotating with an angular frequency ω about the

† Preliminary reports on this work have been given in the proceedings of the international symposium on high-spin states and nuclear structure, Dresden, Sept. 1977, p. 76; and the XVI Winter School Bielsko Biala, Poland, Feb. 1978, p. 551.

†† Present address: Centre d' Études Nucléaires de Grenoble, 85X, F-38041 Grenoble Cédex, France.

x-axis. The lowest eigenstate of $H'(\omega)$ corresponds to an yrast state and the sequence of these states obtained by enlarging ω constitutes the yrast line (actually only the convex parts of it, concave parts must be constructed from excited states of H', ref. [1]).

The natural starting point of the theoretical analysis is the Hartree-Fock-Bogoljubov (HFB) approach to H', which is usually called the (self-consistent) cranking model. There are a number of investigations of the yrast line using this approximation or closely related ones [2-5]. In some cases also non-yrast states have been considered. A central point of all these calculations is a self-consistent determination of the HFB field parameters (nuclear shape and pair field).

In the present publication we face the description of the yrast spectra in a different way. We do not aim at a self-consistent treatment of the HFB field. We calculate the excitation energies of the quasiparticle configurations keeping these parameters fixed to what we think are realistic values. Moreover we do not calculate absolute energies, but only excitation energies with respect to a reference configuration, which will be defined later on. In other words, we are going to interpret the spectrum in the yrast region in terms of quasiparticle configurations of the quasiparticle Routhian, derived from H'. The excitation energies are obtained by simply combining the corresponding quasiparticle energies. Compared to self-consistent HFB calculations a drastic reduction of the computational effort is achieved. Even more importantly, it seems to us that one can present the theoretical results in a very condensed way, viz. diagrams of the quasiparticle energies as functions of ω. This permits consideration of different quasiparticle configurations at the same time, yielding an easily manageable tool for systematizing the experimental spectra. Such an approach is a generalization of the well-known analysis of the properties of non-rotating nuclei in terms of quasiparticle excitations.

In the experiment the energy $E(I)$ as a function of the angular momentum I is measured. These data cannot directly be compared with the quasiparticle spectrum of the Routhian, which represents the energies in the rotating frame as functions of the angular frequency ω. Usually [1-8]) the connection is established by adjusting ω in the calculations so that the constraint $\langle J_x \rangle = I_x$ is fulfilled and transforming the energies from the rotating frame into the laboratory system by means of eq. (1.1). We have chosen the alternative way, namely to represent the experimental energies in the form of the experimental Routhian $E'(\omega)$ defined by

$$E'(\omega) = E(\omega) - \omega I_x(\omega), \tag{1.2}$$

which is the energy in the rotating system. The use of ω instead of I in displaying experimental quantities has become quite familiar since the discovery of backbending (see e.g. refs. [9-12]). The Routhians of the rotational bands near the yrast line may be directly compared with the low-lying part of the quasiparticle spectrum of H'. The main part of this paper is devoted to an investigation of the properties of the ex-

perimental Routhians and their relations to the theoretically calculated quasiparticle energies.

In sect. 2 we sketch the relevant background of HFB theory. Sect. 3 describes the evaluation of the experimental aligned angular momentum and Routhian and sect. 4 defines the reference configuration. Sect. 5 contains a discussion of the parameter choice and in sect. 6 we analyse the experimental Routhian and its derivative, the aligned angular momentum, and compare these quantities with the calculated quasiparticle spectra.

2. Representation of the quasiparticle configurations

The HFB treatment of H' leads to the quasiparticle equations in the rotating system, which have been discussed in many publications [2-5,13,14]). We assume that the nucleus has an axial symmetric shape, z being the symmetry axis. Moreover, symmetry with respect to the xy plane is assumed and only the monopole component of the pair field is supposed to be present. The rotational axis (x-axis) is perpendicular to the symmetry axis, and consequently we deal with collective rotations. The HFB Routhian reads

$$h'_{\text{q.p.}} = h'_{\text{s.p.}} - \Delta(P^+ + P) - \lambda\hat{N}, \tag{2.1}$$

where the single particle Routhian [1,6])

$$h'_{\text{s.p.}} = h_{\text{s.p.}}(\varepsilon) - \omega j_x, \tag{2.2}$$

contains the single particle angular momentum, j_x, and the single particle Hamiltonian, $h_{\text{s.p.}}$, which in our case is the modified harmonic oscillator (MO). It is described in e.g. refs. [6,15]), where ε represents the set of deformation parameters. The operator P^+ creates the pair field (as usual, constant matrix elements are assumed, cf. e.g. ref. [18])), the strength of which is fixed by the gap parameter Δ. The chemical potential, λ, determines the expectation value of the particle number $\hat{N}$.

The eigenfunctions of the HFB Routhian (2.1) are configurations of independent quasiparticles. The quasiparticle states, $|\alpha\mu\rangle$, are solutions of the quasiparticle equations (cf. eq. (2.5)) which have been extensively discussed in refs. [2-5,13,14]). Here we shall only consider their symmetries [14]). The single particle Routhian $h'_{\text{s.p.}}$ is invariant with respect to a rotation $\mathscr{R}_x$ around the x-axis by an angle π,

$$\mathscr{R}_x h'_{\text{s.p.}} \mathscr{R}_x^{-1} = h'_{\text{s.p.}}, \qquad \mathscr{R}_x = \mathrm{e}^{-i\pi j_x}. \tag{2.3}$$

Therefore the single particle states, $|\alpha i\rangle$, of $h'_{\text{s.p.}}$ may be classified according to their symmetry with respect to $\mathscr{R}_x$,

$$\mathscr{R}_x|\alpha i\rangle = \mathrm{e}^{-i\pi\alpha}|\alpha i\rangle. \tag{2.4}$$

Following Bohr and Mottelson [12]) we call α the signature of the state, although they introduced this name not for α but for the whole exponential factor. We prefer α because this is an additive quantity. In the case of single particle states, α takes the values $\pm\frac{1}{2}$. The only further symmetry is the parity, π. The inclusion of the monopole pairing field in eq. (2.1) does not destroy these symmetries. Using as a basis the eigenfunctions of the single particle Hamiltonian $h_{\text{s.p.}}$ with good signature, the quasiparticle equations read

$$\mathscr{H}'_{\alpha}|\alpha\mu\rangle = E'_{\alpha\mu}|\alpha\mu\rangle, \tag{2.5}$$

with

$$\mathscr{H}'_{\alpha} = \begin{pmatrix} (\varepsilon-\omega j_x-\lambda)_{\alpha i\alpha i'} & \Delta \\ \Delta & -(\varepsilon-\omega j_x-\lambda)_{-\alpha i-\alpha i'} \end{pmatrix}, \tag{2.6}$$

$$|\alpha\mu\rangle = \begin{pmatrix} U^{\alpha\mu}_{\alpha i} \\ V^{\alpha\mu}_{-\alpha i} \end{pmatrix}. \tag{2.7}$$

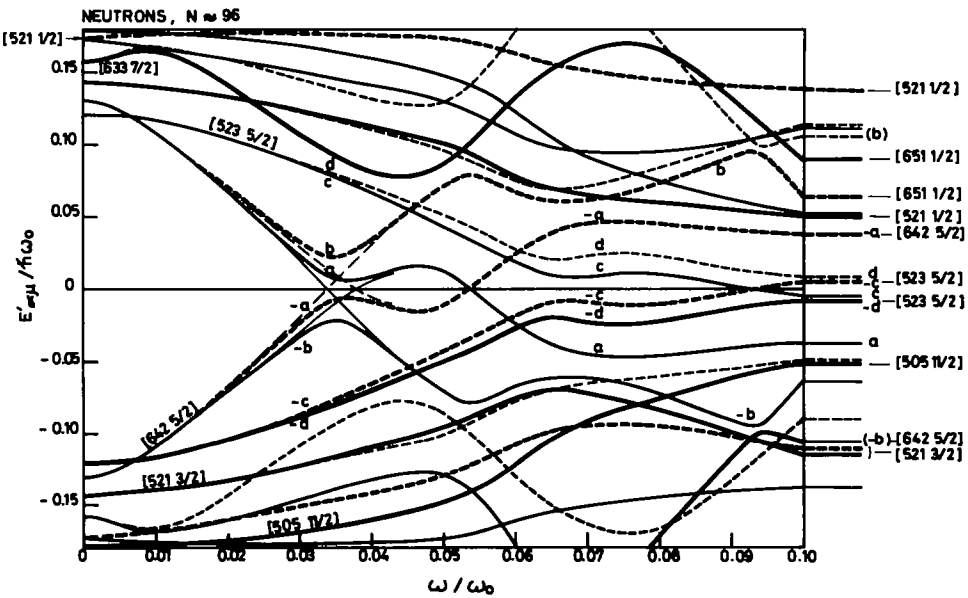

Fig. 1. The quasiparticle energies for neutrons plotted as functions of the rotational frequency. Levels with $\alpha = \frac{1}{2}$ are drawn with solid lines and those with $\alpha = -\frac{1}{2}$ are dashed. The thin full and long dashed lines show the pure levels obtained by eq. (4.1). For each pair of conjugate states a label, $[Nn_z\Lambda\Omega]$, is indicated on either the level with positive energy or the one with negative energy, depending on whether the corresponding single-particle level (for $\omega = 0$) is situated above or below the Fermi surface. For $\omega/\omega_0 < 0.05$ the following parameters have been used: $\varepsilon_2 = 0.26$, $\Delta = 0.12\ \hbar\omega_0$ (these two values are the same in all diagrams shown in this paper) and $\lambda = 6.485\hbar\omega_0$ corresponding to 96 neutrons. Above $\omega = 0.05\omega_0$ the gap Δ is assumed to decrease linearly from $0.12\hbar\omega_0$ at $\omega = 0.05\omega_0$ to zero at $\omega = 0.10\omega_0$ and λ is chosen such that $N = 96$ for the vacuum configuration. The single particle levels calculated at $\omega = 0.10\omega_0$ are shown to the right. Since some of the levels interact and exchange their character, the quantum numbers given to a certain level are not always the same at $\omega = 0.10\omega_0$ as at $\omega = 0$, cf. e.g. the level marked *b*.

The solutions of these equations must be found numerically. The quasiparticle states can then be classified with respect to α and π, and in our case of the MO potential also with respect to N, the total number of oscillator quanta, since we neglect couplings between different N-shells. Fig. 1 shows a diagram of the quasiparticle levels as functions of the angular frequency ω. In order to invoke a full classification, we label each level with the asymptotic quantum numbers of the MO potential and indicate the sign of its energy. The MO quantum numbers are of course only relevant for $\omega = 0$, but we also use them for the continuations of the levels to finite values of ω. The energy scale $\hbar\omega_0$ is defined in ref. [15]).

The usual way [2-5,13,14]) to construct quasiparticle configurations from the quasiparticle states $|\alpha\mu\rangle$ (we denote only the signature explicitely) is to consider only the solutions $E'_{\alpha\mu} > 0$ as the physical ones, which define the quasiparticle operators $\beta^+_{\alpha\mu}$ and the vacuum. The one-, two-, ... quasiparticle configurations are obtained by acting with one, two, ... operators $\beta^+_{\alpha\mu}$ on the vacuum, $|\text{vac}\rangle$.

(i) *The excitation energy with respect to the vacuum is the sum of the energies $E'_{\alpha\mu}$ of the occupied physical states. The same is true for other additive quantities like angular momentum, signature etc.* This formulation is the most convenient one as long as the physical levels do not cross with the "unphysical" (negative energy) ones. The situation becomes more complicated (see e.g. refs. [13,16])) when there are crossings as in fig. 1 at $\omega = 0.054\omega_0$ and especially in the case of the crossing with finite interaction between the levels occurring at $\omega = 0.036\omega_0$. In such cases it is much easier to cope with the underlying physics if one considers both positive and negative energy solutions.

This can be done by means of the occupation number representation for quasiparticles (cf. ref. [17])) which is an equivalent alternative to the introduction of quasiparticle operators. The formalism is somewhat different from the usual occupation number representation of fermions. The quasiparticle occupation numbers $n_{\alpha\mu}$ are the eigenvalues of the generalized density matrix

$$\mathscr{K}_\alpha(\alpha_t A) = \langle \alpha_t A | \begin{pmatrix} c^+_{\alpha i} c_{\alpha i'} & c^+_{\alpha i} c^+_{-\alpha i'} \\ c_{-\alpha i} c_{\alpha i'} & c_{-\alpha i} c^+_{-\alpha i'} \end{pmatrix} | \alpha_t A \rangle . \tag{2.8}$$

The operator $c^+_{\alpha i}$ creates a particle in the state $|\alpha i\rangle$. The state $|\alpha_t A\rangle$ represents a quasiparticle configuration, which is classified by its total signature α_t and the necessary additional quantum numbers A. The density matrix $\mathscr{K}_\alpha$ is diagonal in the basis of quasiparticle states $|\alpha\mu\rangle$. Its eigenvalues, the quasiparticle occupation numbers $n_{\alpha\mu}$, take the values 0 and 1. We refer to the corresponding levels as "free" and "occupied", respectively.

As seen in fig. 1, there is a further symmetry of the quasiparticle states (cf. refs. [14,17])). For each state $|\alpha\mu\rangle$ there is a conjugate state $|-\alpha\mu\rangle$, which is related to the former one by

$$E'_{-\alpha\mu} = -E'_{\alpha\mu}. \tag{2.9}$$

The corresponding transformation between the vectors of the conjugate states leads to the following relation for the occupation numbers:

(ii) *If a level $E'_{\alpha\mu}$ is occupied, its conjugate partner, $E'_{-\alpha\mu}$, obtained by reflexion in the line $E' = 0$, is free.* This rule excludes a large number of possible combinations of the $n_{\alpha\mu}$. However, this restriction just accounts for the fact, that there are twice as many quasiparticle states $|\alpha\mu\rangle$ as single-particle states $|\alpha i\rangle$. The double dimension is also the reason for a second pecularity that concerns expectation values (cf. ref. [17])):

(iii) *An additive quantity (energy, angular momentum, signature, particle number etc.) is equal to one-half of the sum of the contributions from all occupied levels (including the negative ones).* The occurance of the factor $\frac{1}{2}$ may be traced back to the generalized density matrix (2.8). In order to express the expectation value of, say J_x, through the occupation numbers $n_{\alpha\mu}$ one must write it as the trace over the generalized density matrix, like

$$\langle\alpha_t A|J_x|\alpha_t A\rangle = \tfrac{1}{2}\sum_{\alpha} \mathrm{tr}\,(\mathscr{J}_\alpha \mathscr{K}_\alpha). \tag{2.10}$$

The matrix $\mathscr{J}_\alpha$ is the angular momentum in the double dimensional representation (2.8)

$$\mathscr{J}_\alpha = \begin{pmatrix} j^x_{\alpha i \alpha i'} & 0 \\ 0 & -j^x_{-\alpha i -\alpha i'} \end{pmatrix}. \tag{2.11}$$

The factor $\frac{1}{2}$ appears because $\mathscr{K}_\alpha$ contains the ordinary density matrix twice ($\langle c^+_{\alpha i} c_{\alpha i'}\rangle$ and $\langle c_{-\alpha i} c^+_{-\alpha i'}\rangle$). Changing to the quasiparticle states as basis makes $\mathscr{K}_\alpha$ diagonal:

$$\langle\alpha_t A|J_x|\alpha_t A\rangle = \tfrac{1}{2}\sum_{\alpha\mu} n_{\alpha\mu}\langle\alpha\mu|j_x|\alpha\mu\rangle, \tag{2.12}$$

The angular momenta $\langle\alpha\mu|j_x|\alpha\mu\rangle$ of the quasiparticle states are the diagonal elements of the matrix $\mathscr{J}_\alpha$, transformed to the basis $|\alpha\mu\rangle$.

The above arguments may be repeated for other single-particle operators like the total signature and the energy E' calculated as the expectation value of the HFB Routhian $h'_{\mathrm{q.p.}}$ (eq. (2.1)). The energy of the states $|\alpha\mu\rangle$ is, of course, the quasiparticle energy, $E'_{\alpha\mu}$, shown in the level diagrams. This way of calculating the total energy neglects the interaction between the quasiparticles. It makes only sense if we consider the *excitation energy* of a configuration relative to some reference configuration, |ref⟩, and if the number of excited quasiparticles is not too large.

The configuration with the lowest energy corresponds to the one with all negative energy levels filled. This is the vacuum configuration, |vac⟩, needed in the quasiparticle operator representation. At high frequencies, where positive and negative levels cross, this definition must be slightly modified. We then define the vacuum as the configuration with *even* particle number that has the lowest energy (cf. below and ref. [2])).

The relation between the quasiparticle and the occupation number representation is very simple. Creating a quasiparticle $\alpha\mu$, i.e. making the state $\beta^+_{\alpha\mu}|\text{vac}\rangle$ is equivalent to changing the occupation numbers of the vacuum so that the level $\alpha\mu$ ($E'_{\alpha\mu} > 0$) becomes occupied and the conjugate level $-\alpha\mu$ ($E'_{-\alpha\mu} < 0$) becomes free. The factor $\frac{1}{2}$ in the expectation values ensures identical results. The generalization to many quasiparticle configurations is obvious.

The distinguished role of the vacuum introduces an asymmetry in the description of quasiparticle configurations by means of quasiparticle operators. The choice of the vacuum configuration as a reference can only be justified by practical reasons, namely if one wants to refer to the state with minimal energy. The vacuum has the disadvantage that its structure drastically changes in the regions where the positive and negative energy levels cross each other. For the analysis of the yrast spectra in the angular momentum region up to about $25\hbar$, we found the ground state configuration to be a more convenient reference. Therefore we prefer the flexible occupation number representation that allows us to speak about one-, two-, ... quasiparticle excitations with respect to any reference configuration chosen in the particular case.

(iv) *Since we only calculate relative quantities, we define a* **reference configuration** *for which we choose the ground configuration (g-configuration).* At low ω the g-configuration corresponds to all levels $E'_{\alpha\mu} < 0$ occupied. At higher ω, where positive and negative energy levels cross each other, the g-configuration is defined as the continuation of the previous structure (see sect. 3), because it contains only collective rotational energy and its structure changes gradually in the crossing region. Obviously, at low frequencies the g and vacuum configurations are identical and there it might be most convenient to refer to the quasiparticle operators.

There is a useful property of the quasiparticle energies $E'_{\alpha\mu}$, which follows from the stationarity of the quasiparticle solutions:

$$-\frac{\mathrm{d}E'_{\alpha\mu}}{\mathrm{d}\omega} = \langle\alpha\mu|\, j^x|\alpha\mu\rangle. \tag{2.13}$$

(v) *For a quasiparticle level $E'_{\alpha\mu}(\omega)$ the negative slope is equal to its angular momentum component along the x-axis.*

There is an important selection rule that concerns the total angular momentum I

$$I = \alpha_i \bmod 2. \tag{2.14}$$

It is not generally valid, but applies to cases where the rotational symmetry around the x-axis is sufficiently strongly violated, so that collective rotation about this axis is possible. Eq. (2.14) reflects the well-known symmetrization of the wave functions in the rotor model, which derives from the fact that, for the class of shapes that we are considering, the intrinsic frame of reference is only determined up to a rotation of π about the intrinsic axis. Accordingly we associate with a certain con-

figuration $|\alpha_t A\rangle$ (considered as a function of ω) a rotational band with the intrinsic structure defined by A and the angular momenta $I = \alpha_t + 2n$, where n is an integer number. A more detailed discussion of this point is given in refs. [12,18,19]).

The total signature decides also, whether the particle number is odd or even. This follows immediately from the relation

$$\mathscr{R}_x^2(\pi) = e^{-2\pi i j_x} = e^{-i\pi\hat{N}}. \tag{2.15}$$

Thus we may summarize:

(vi) *The total signature α_t of a configuration restricts its angular momentum to $I = \alpha_t \bmod 2$ and determines whether the system has odd or even particle number, $N = 2\alpha_t \bmod 2$.*

The parity of a configuration is given by the following rule:

(vii) *The parity of the g-configuration is $\pi = +$. The parity of any excited configuration is the product of the parities of the levels, which are occupied in the excited configuration but free in the g-configuration.*

3. The experimental Routhian and aligned angular momentum

In order to calculate the experimental Routhian (eq. (1.2)) the rotational frequency has to be determined. This can be done by means of the canonical relation

$$\omega = \frac{dE(I)}{dI_x}, \tag{3.1}$$

approximating the differential quotient by a quotient of finite differences

$$\omega(I) = \frac{E(I+1) - E(I-1)}{I_x(I+1) - I_x(I-1)}. \tag{3.2}$$

Due to the symmetry properties, as described by the signatures, we always restrict ourselves to sequences with $\Delta I = 2$, when defining a rotational band. In eq. (3.2) we use the classical relation

$$I_x(I) = \sqrt{(I+\tfrac{1}{2})^2 - K^2}, \tag{3.3}$$

in order to take into account the projection K of the angular momentum onto the symmetry axis. The value of K is set equal to the angular momentum of the band head †.

† In cases when the angular momentum of the lowest observed state in a band is not given by the K-value, as for the strongly decoupled $i_{13/2}$ bands, we use the K that can be read out of the calculated level diagram.

This choice was dictated by the desire to use only experimental data in the analysis of the spectra. Although K is only well defined in the limit $\omega = 0$, the procedure may be justified by the fact that K-mixing is only important when I_x does not depend very much on the exact value of K (i.e. K small or $I \gg K$). Concerning the use of $(I+\frac{1}{2})$, cf. ref. [12]) and below.

A careful definition of $\omega(I)$ is the following. Any transition $I+1 \rightarrow I-1$ within a rotational band determines, via eq. (3.2), one value of ω that is ascribed to the angular momentum I, which is the mean value of the two angular momenta involved in the transition. This procedure provides a discrete set of points $\omega(I)$. The continuous function $\omega(I)$ and its inverse $I(\omega)$ are defined as interpolations of the discrete set. The function $I_x(\omega)$ is defined by means of eq. (3.3) by substituting I with $I(\omega)$.

The experimental Routhian (1.2) is defined by means of

$$E'(I) = \tfrac{1}{2}(E(I+1)+E(I-1))-\omega(I)I_x(I), \tag{3.4}$$

where the average value of $E(I-1)$ and $E(I+1)$ is used as an approximation for $E(I)$, which is the energy at the intermediate value I of the angular momentum. This expression combined with $\omega(I)$ provides again a discrete set of points $\{E'(I), \omega(I)\}$ and the continuous function $E'(\omega)$ is defined by interpolation.

Let us now introduce the relative quantities

$$e'(\omega) = E'(\omega)-E'_g(\omega), \tag{3.5}$$

$$i(\omega) = I_x(\omega)-I^x_g(\omega), \tag{3.6}$$

where $E'_g(\omega)$ and $I^x_g(\omega)$ are, respectively, the Routhian and the x-component of the angular momentum of the reference configuration. Since the reference quantities are only defined for even-even nuclei, we have to use a slightly modified definition for odd-mass nuclei. We then use as a reference the mean values of $E'_g(\omega)$ or $I^x_g(\omega)$ calculated from the g-bands of the two even-even neighbours. Notice that the energy of the odd-mass nucleus counted from the even neighbours includes the even-odd mass difference. Thus, for an odd-mass nucleus, the Routhian reads

$$e'(A,\omega) = E'(A,\omega)+\Delta-\tfrac{1}{2}[E'_g(A+1,\omega)+E'_g(A-1,\omega)], \tag{3.7}$$

where A is the (odd) mass number and Δ the even-odd mass difference.

The reason for introducing e' and i is that we are not interested in the absolute values, but rather in their differences between various configurations, since these are the quantities, which can be read from the quasiparticle energy diagrams. We do not aim at a calculation of E'_g and I^x_g, but take these quantities from the experiment. To avoid confusion we are using capital letters (E', I etc.) to describe the total value of a quantity, while small letters (e', i etc.) are used for the value of a quantity relative to the reference.

4. Definition of the reference

As in our previous work [20]) we use the energies of the ground state band (g-band) of an even nucleus as the reference. Therefore the Routhian $e'(\omega)$ is the excitation energy in the rotating frame relative to the g-band and $i(\omega)$ is the magnitude of the aligned angular momentum relative to the g-band.

In the level diagrams the g-configuration † corresponds to the one with all levels $E'_{\alpha\mu} < 0$ occupied as long as the positive and negative levels are well separated. There, it also coincides with the vacuum. In accordance with the experiment the g-configuration has the signature $\alpha_i = 0$ and the parity $\pi = +$.

To each quasiparticle configuration we ascribe a rotational band. The crossings of the quasiparticle levels reflect the crossings of rotational bands. Naturally, the configurations that preserve the character of the wave function through the crossing point, i.e. those obtained by a smooth continuation of the levels, must be connected to rotational bands.

In the region $\omega \gtrsim 0.03\omega_0$ the positive and negative quasiparticle levels cross each other. This means that the g-band crosses with other bands and is no longer the yrast line. Nevertheless we use it as the reference. Actually the first point where, in fig. 1, the positive and negative levels come into contact is not a real crossing but the quasi-crossing of the levels a and $-b$ as well as b and $-a$ at $\omega = 0.036\omega_0$. Due to the small interaction the states repel each other and interchange their character. The configuration with the levels a, b occupied and $-a$, $-b$ free has a wave function similar to the g-configuration before the crossing. We consider it as the continuation of the g-configuration and use it as reference. In the region where the mixing between the quasiparticle states is substantial we must reconstruct the pure g-configuration. As proposed in ref. [20]), this can be achieved with sufficient accuracy by assuming an ω-independent interaction V between the two states of equal signature. The distance $\Delta e'_0$ between the pure levels is then given by the known distance $\Delta e'$ between the mixed ones

$$\Delta e'_0 = \sqrt{(\Delta e')^2 - (2V)^2}, \tag{4.1}$$

where $2V$ is the minimal distance of the interacting states. The pure levels obtained in this way are indicated by the thin lines in fig. 1. The g-configuration corresponds to an occupation of the pure states connecting the low frequency parts of $-a$ and $-b$ with b and a.

The next crossings that appear at $\omega = 0.045\omega_0$ and $\omega = 0.052\omega_0$ may be treated in the same way. This would provide a continuation of the g-configuration to still higher frequencies. The proposed reconstruction of the pure g-configuration relies on two assumptions. One, that only two levels are mixed at the crossing point and, the other, that the interaction matrix element V does not depend on ω. These as-

† We use the word configuration when we refer to a certain occupation of the quasiparticle levels, whereas the word band is used in connection with the experimentally observed rotational bands.

sumptions are well fulfilled when the interaction is small. If it is strong like it is in fig. 3, the interaction region covers a larger interval of ω for which the assumption of a constant interaction is less justified. Moreover the adjacent crossings are not well separated as seen by the incipient perturbation of the pure levels in fig. 1. Thus, in the case of strong interaction our two level treatment may cause noticeable errors in the reference energies. Fig. 1 seems to suggest that the accuracy could be improved by treating the first three crossings simultaneously with a four level expression. However, in the region $\omega > 0.05\omega_0$ the g-configuration loses its identity and is no longer a useful reference.

In the backbending region the g-band crosses the s-band (for a more careful discussion see subsect. 6.3 and refs. [12, 20]). This crossing is the experimental counterpart of the level crossing at $\omega = 0.036\omega_0$ in fig. 1.

Only in exceptionel cases is the g-band measured beyond the crossing. In order to obtain the reference energies near and above the crossing we are forced to extrapolate the low frequency parts of $E'_g(\omega)$ and $I^x_g(\omega)$. We use

$$I^x_g(\omega) = (\mathscr{J}_0 + \omega^2 \mathscr{J}_1)\omega, \tag{4.2}$$

where $\mathscr{J}_0$ and $\mathscr{J}_1$ are constants. This corresponds to the Harris formula [21]) of rotational spectra, which is equivalent to the VM1 expression [22]). The constants $\mathscr{J}_0$ and $\mathscr{J}_1$ are normally taken from the linear part of $\mathscr{J}_{\text{eff}} = I^x_g/\omega$ as function of ω^2, which is the usual backbending plot for the yrast line (compare, however, sect. 5). Integrating eq. (4.2) we obtain the reference Routhian as

$$E'_g(\omega) = -\int I^x_g(\omega)\mathrm{d}\omega = -\tfrac{1}{2}\omega^2 \mathscr{J}_0 - \tfrac{1}{4}\omega^4 \mathscr{J}_1 + \tfrac{1}{8}\hbar^2/\mathscr{J}_0. \tag{4.3}$$

The three-dimensional character of the rotation is reflected by the quasiclassical expression $(I+\frac{1}{2})^2$ for the square of the angular momentum. Hence, for the $K = 0$ g-band we obtain from eq. (3.3)

$$I^x_g = I_x(K = 0) = I + \tfrac{1}{2}\hbar. \tag{4.4}$$

This leads to $I^x_g(I = 0) = \frac{1}{2}\hbar \neq 0$. The integration constant in eq. (4.3) is chosen such that the ground state energy $E'_g(I = 0)$ is equal to zero (neglecting terms proportional to ω^4).

The g-band shows the typical pattern of a collective rotation. This is in accordance with the fact that in the g-configuration the angular momentum is composed of small contributions from many occupied quasiparticle states. Therefore we interpret the reference quantities I^x_g and E_g as the collective angular momentum and collective rotational energy respectively. The relative quantities e' and i tell us which energy and angular momentum the nucleus carries in addition to the collective part of these

quantities. This simple concept is the reason why the g-configuration seems to us to be a suitable reference. Notice that $i(\omega)$ differs from the "alignment plot" used by the Jülich group (see e.g. ref. [24])) which shows the total angular momenta of the canonical single particle states.

5. Choice of parameters

In most cases the Harris parameters $\mathcal{J}_0$ and $\mathcal{J}_1$ have been chosen to reproduce the linear part of the function $\mathcal{J}_{\text{eff}}(\omega^2)$. There is, however, a complication which arises from the fact that $\mathcal{J}_1$ strongly increases if N approaches 90. This reflects the increasing ω-dependance of the deformation for these light nuclides (see ref. [24])). Extrapolating the steep slope of the reference moment of inertia at low frequencies has the consequence that $i(\omega)$ becomes a decreasing function at large frequencies. It is evident that this linear growth of $\mathcal{J}_{\text{eff}}(\omega^2)$ cannot continue to very high frequencies. The function should level off, remaining below the rigid body value. In order to improve the representation of $\mathcal{J}_{\text{eff}}(\omega^2)$ over the entire ω-interval of interest, we choose the reduced value $\mathcal{J}_1 = 90\ \text{MeV}^{-3} \cdot \hbar^4$ for the nuclides around $N = 90$ and determine $\mathcal{J}_0$ such that the Harris line intersects $\mathcal{J}_{\text{eff}}(\omega^2)$ at about the middle of its linear part. With this choice, $i(\omega)$ is always either an increasing function of ω or for the strongly decoupled $i_{13/2}$ bands remains nearly constant (see subsects. 6.2 and 6.6). Clearly one could improve this somewhat crude procedure by a nonlinear parametrization of $\mathcal{J}_{\text{eff}}(\omega^2)$. The parameters $\mathcal{J}_0$ and $\mathcal{J}_1$ are indicated in figs. 2, 3, 5, 7, 9 and 12.

The value of K used in eq. (3.3) coincides for one quasiparticle bands with Ω of the assigned MO quantum number $[Nn_z\Lambda\Omega]$. For many quasiparticle bands it is a combination of the Ω-values of the assigned MO labels.

The theoretical quasiparticle energies depend on the gap Δ, the chemical potential λ and the deformation parameters, for which we have to make a choice.

We assume an axial deformation, the symmetry axis being z. We use the quadrupole deformation $\varepsilon_2 = 0.26$ and no hexadecapole deformation $\varepsilon_4 = 0$. This is the ground state shape for $A \approx 165$, but we have found that the diagrams calculated for this deformation can be successfully used for the considered mass region $157 \leqq A \leqq 169$. For the lightest nuclides a smaller ε_2 and a slightly negative ε_4 would be optimal [15]). However, the resulting level shifts are not very dramatic because the separate changes due to ε_2 and ε_4 partly compensate each other. The choice of a constant axial deformation for the well deformed nuclei in the middle of the rare earth region is supported by the measurements of the E2 lifetimes (see ref. [11])). Also calculations of the deformation energies show only small changes of the equilibrium shape for $I \leqq 30\hbar$ and $A \approx 165$ (see refs. [1,6,8])).

In this paper we always use the gap parameter $\Delta = 0.12\hbar\omega_0$ independent of ω. This value represents an average of the experimental even odd mass differences for

the Er and Yb isotopes which we are concerned with †. The choice of a constant Δ may seem surprising. However, the success in interpreting the data indicates that this should be a reasonable value. Especially, the existence of the s-band and the aligned bands in odd mass nuclei (cf. below) is only compatible with a strong pairing up to a frequency $\hbar\omega \approx 0.3$ MeV. Moreover, we calculated the absolute pair correlation energy using particle number projection [25,26]) and performed a minimization with respect to the strength of the pair field. We found strong pair correlations in the g-configuration up to angular momenta of $I \approx 20\hbar$. This stability of the pair field is mainly due to the corrections for particle number conservation, which increase the correlation energy. It seems therefore reasonable that the excitation energies with respect to the g-configuration may be reproduced by a Δ close to the ground state value. The gap Δ is also not a very critical parameter. Variations of the order of 20% do not drastically change the structure of the level diagrams.

The choice of λ is not problematic, because the expectation value of the particle number depends weakly on the frequency. Keeping λ fixed within the usually considered interval of $\omega < 0.05\omega_0$ we found changes of the order of a half unit. A better accuracy is not necessary for the comparison of the quasiparticle levels with the experimental Routhians. Therefore we use the value of λ that gives the correct particle number for $\omega = 0$.

The parameters κ and μ of the MO potential are the "$A = 165$ values" of ref. [15]).

6. Analysis of experimental spectra in the rare earth region

In this section we analyse the rotational bands of rare earth nuclei with proton numbers $68 \leqq Z \leqq 70$ and neutron numbers $89 \leqq N \leqq 99$. The rules (i)–(vii) given in sect. 2 may be considered as the "users' instructions" for the analysis of the experimental bands in terms of quasiparticle configurations.

We need a simple way of labelling the excited configurations. The convention is used that the MO quantum numbers and the signature of the occupied levels with $E'_{a\mu} > 0$ are quoted in squared brackets: $[Nn_z\Lambda\Omega\alpha]$, ... In the case where this might lead to confusion we use instead the labels $a, b, \ldots$ indicated in the diagrams. (The conjugate levels are denoted by $-a, -b, \ldots$.)

6.1. ONE-QUASIPARTICLE CONFIGURATIONS IN A NUCLEUS WITH ODD NEUTRON NUMBER

Example: ^{167}Yb. The Routhians for the observed bands [27,28]) of ^{167}Yb are shown in fig. 2. Since the frequency, ω, is relatively low only one quasiparticle states are seen. Accordingly, the energies are directly comparable with the levels in the upper half of the quasiparticle energy diagram shown in fig. 1. The total signature may take

† Note, however, that in the experimental diagrams, we do not use the average value of Δ, but the experimental odd-even mass difference, determined individually for each nucleus.

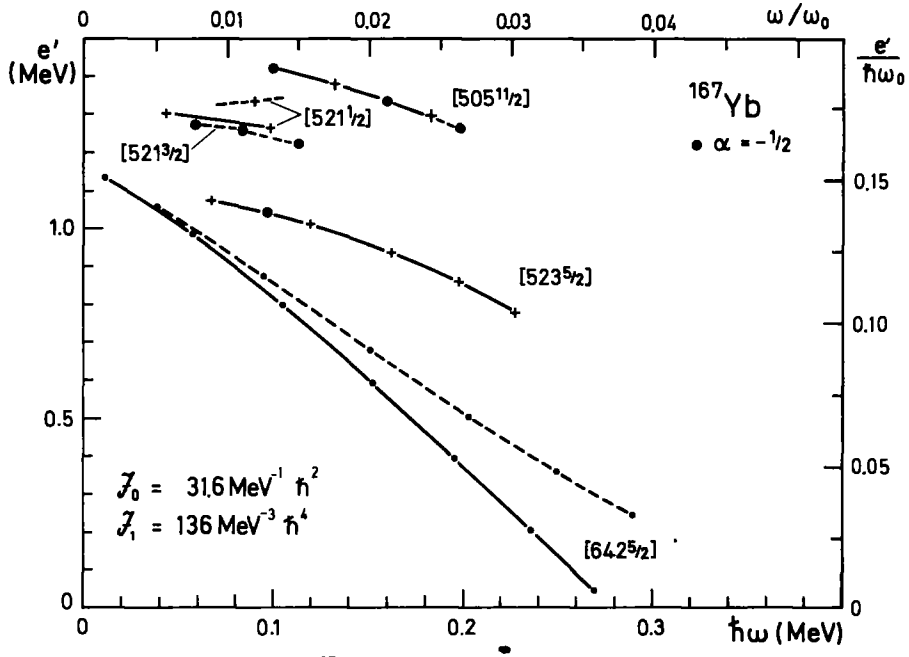

Fig. 2. Experimental Routhians for ^{167}Yb. As in all figures showing the experimental Routhians of odd mass nuclei, we use solid lines if $\alpha = \frac{1}{2}$ and dashed lines if $\alpha = -\frac{1}{2}$. If the two signiatures are degenerate, a special symbol, indicated in each figure, is used for $\alpha = -\frac{1}{2}$. The scale of all figures is such that the slopes can be directly compared to the slopes of the corresponding theoretical quasiparticle levels. The parameters $\mathcal{J}_0$ and $\mathcal{J}_1$ of the reference Routhian are also indicated. The value of K coincides with Ω in the MO labels $[Nn_z\Lambda\Omega]$. The scale $\hbar\omega_0$ is converted into MeV using the relation $\hbar\omega_0 = 41$ MeV $A^{-\frac{1}{3}}$ which is sufficiently accurate for our purposes.

the values $\alpha_t = \pm\frac{1}{2}$ and the angular momentum is $I = \frac{1}{2}, \frac{5}{2}, \frac{9}{2}$ etc. if $\alpha_t = +\frac{1}{2}$, or $I = \frac{3}{2}, \frac{7}{2}, \frac{11}{2}$ etc. if $\alpha_t = -\frac{1}{2}$.

The two lowest states are $[642\frac{5}{2}; \alpha = \frac{1}{2}]$ and $[642\frac{5}{2}; \alpha = -\frac{1}{2}]$, which show a clear signature splitting. Both levels are descending rapidly with an almost constant slope, corresponding to an aligned angular momentum $i = -\mathrm{d}e'/\mathrm{d}\omega \approx 4.5\hbar$ and $3.4\hbar$ for the $\alpha = \frac{1}{2}$ and $\alpha = -\frac{1}{2}$ signature, respectively (determined for the interval 0.1 MeV $\leqq \hbar\omega \leqq$ 0.2 MeV). The agreement with the theoretical quasiparticle levels is good although the energetic signature splitting is about a factor of 3 larger in experiment than calculated. The slopes of calculated levels correspond to $i = 4.1\hbar$ and $3.7\hbar$, respectively.

At $\hbar\omega \approx 0.037\hbar\omega_0 \approx 0.28$ MeV the levels $E'_{[642\frac{5}{2};\,\alpha=\pm\frac{1}{2}]} > 0$ interact with the negative solutions. This interaction is closely related to the backbending phenomenon (see subsect. 6.3). In the case of the odd neutron configuration $[642\frac{5}{2}; \alpha = \frac{1}{2}]$ the levels $-b$ and a are occupied while b and $-a$ are free. The contribution of these levels to the total energy will therefore be $\frac{1}{2}(E'_{-b}+E'_a)$, which is equal to the same expression for the pure levels shown by the thin lines. Therefore the interaction does not show

up and the energy goes smoothly through the region of interaction. This expresses of course that we deal with identical fermions, i.e. a canonical transformation including only the levels a and $-b$ does not change the state. The fact is commonly stated as "the blocking of the state by the odd particle prevents backbending". The situation for $[642\frac{5}{2}; \alpha = -\frac{1}{2}]$ is analogous.

The g-configuration used as reference corresponds to the occupation of the pure states, which interpolate between the levels a and $-b$ and between b and $-a$ through the interaction region. Therefore, the experimental analysis shows a picture without interaction, i.e. the experimental Routhian of the configuration $[642\frac{5}{2}; \frac{1}{2}]$† crosses $e' = 0$ without any perturbation and it must be compared with the corresponding pure level.

For the $[642\frac{5}{2}; \frac{1}{2}]$ band the experimental crossing point with the line $e' = 0$ lies at $\hbar\omega = 0.28$ MeV and agrees well with the value read from the theoretical diagram, which is $\hbar\omega = 0.26$ MeV.

The $[523\frac{5}{2}; \pm\frac{1}{2}]$ bands start with a small slope, which increases with the frequency in good correspondence to the theory. Their continuations seem to cross the $[642\frac{5}{2}; \pm\frac{1}{2}]$ bands at roughly the same frequency as in the theory.

Also for the higher lying levels there is a good agreement between experiment and theory. Notice especially the $[521\frac{1}{2}; \pm\frac{1}{2}]$ bands, which show a large signature splitting at small frequencies. These bands form together a "$K = \frac{1}{2}$ band". The Routhians of the two signatures have a finite slope $\pm\frac{1}{2}a$ in the limit $\omega = 0$, where a is the so-called decoupling parameter [for definition see e.g. ref. [18]) eq. (4.60)].

For the $[505\frac{11}{2}; \pm\frac{1}{2}]$ bands the energy relative to the ground state is not exactly known, and we have somewhat arbitrarily placed them at an energy where we expect them to lie.

For ^{167}Yb, as well as for the other odd mass nuclei treated in this paper, we include into the experimental energies the odd-even mass difference (eqs. (2.92, 2.93) ref. [18])) as determined from refs. [29,30]). This is in accordance with our choice of Δ in the calculations of the level diagrams. The steep slope of the lowest $i_{\frac{13}{2}}$ levels is a consequence of the pair correlations. We found that a reduction of Δ to 0.06 and $0.03\hbar\omega_0$ decreases the theoretical i for the level $[642\frac{5}{2}; \frac{1}{2}]$ from $4.1\hbar$ to $3\hbar$ and $1.7\hbar$, respectively. Compare also figs. 7 and 24 in ref. [6]) showing $i(\omega)$ for the case $\Delta = 0$. As seen there, the levels emerging from the middle of the $i_{\frac{13}{2}}$ multiplet carry very little aligned angular momentum in the considered interval of ω. Thus, in order to reproduce the experimental values of i, a gap Δ comparable with the ground state value is necessary.

The possibility that the quasiparticle levels enter the gap region when the strength parameter Δ of the pairfield is still large represents the nuclear analog to the phenomenon of gapless superconductivity, which appears in metals with paramagnetic impurities [31]). The analogy was first pointed out in refs. [32,33]).

† From now on, we write $[642\frac{5}{2}; \pm\frac{1}{2}]$ instead of $[642\frac{5}{2}; \alpha = \pm\frac{1}{2}]$ etc. The last number always indicates α.

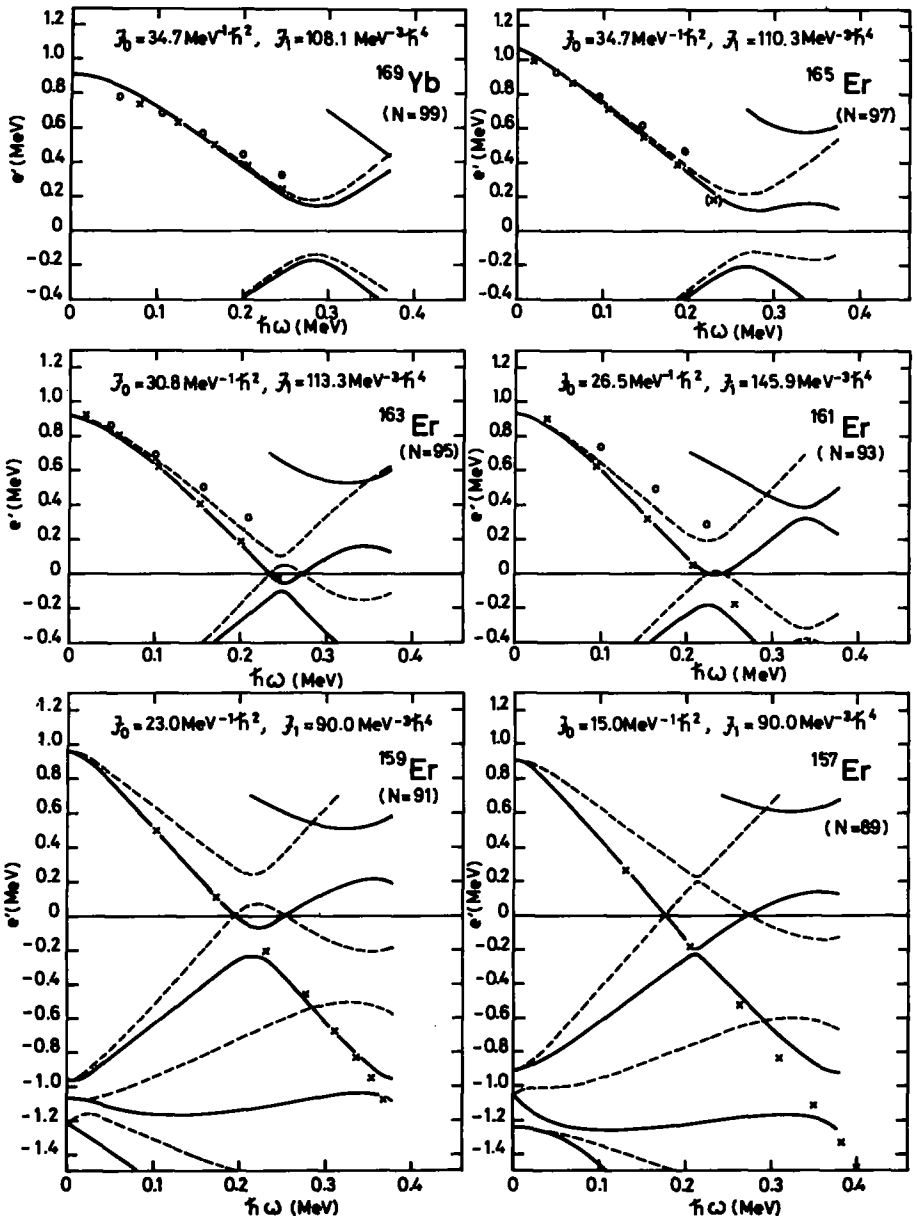

Fig. 3. The theoretical $i_{13/2}$ quasineutron levels closest to the Fermi surface for neutron numbers $N = 89, 91, 93, 95, 97$ and 99. The values of K used in the analysis are $\frac{1}{2}, \frac{3}{2}, \frac{3}{2}, \frac{5}{2}, \frac{5}{2}$ and $\frac{7}{2}$ respectively. Solid lines indicate $\alpha = \frac{1}{2}$ and dashed lines $\alpha = -\frac{1}{2}$. The corresponding experimental Routhians are also indicated (crosses if $\alpha = \frac{1}{2}$, circles if $\alpha = -\frac{1}{2}$). They have been calculated for the Er-isotopes except for $N = 99$, where ^{169}Yb has been used. In order to facilitate a comparison of the slopes and the signature splittings, the experimental Routhians have been shifted up or down so that the $\alpha = \frac{1}{2}$ level coincides with the corresponding calculated level at $\hbar\omega = 0.15$ MeV.

6.2. THE SYSTEMATICS OF THE $i_{13/2}$ BAND IN ODD MASS Er ISOTOPES

In fig. 3 we show the experimental Routhians of the $i_{13/2}$ bands for $^{157-165}$Er [refs. [34,35])] and ^{169}Yb [ref. [36])], i.e. for neutron numbers 89–99. (For $N = 99$ we have

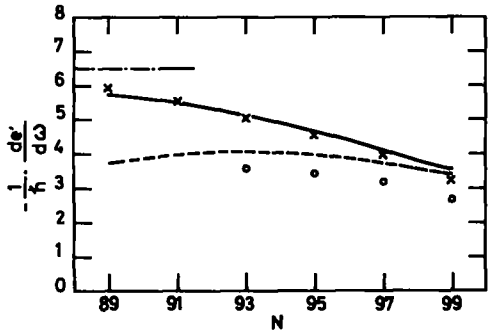

Fig. 4. The aligned angular momentum of the $i_{13/2}$ band at $\hbar\omega \approx 0.15$ MeV as function of the neutron number. The values of the angular momentum have been determined from the slopes of the corresponding quasiparticle levels or experimental Routhians shown in fig. 3. The calculated values are shown by the solid ($\alpha = \frac{1}{2}$) and the dashed ($\alpha = -\frac{1}{2}$) lines. The experimental values are displayed by the crosses ($\alpha = \frac{1}{2}$) and the circles ($\alpha = -\frac{1}{2}$).

chosen ^{169}Yb, since too few states are known in ^{167}Er.) In the same diagrams we have also drawn the $i_{13/2}$ quasiparticle levels. This sequence of isotopes shows some systematics.

(i) For $N = 99$ the signature splitting is very small. With decreasing neutron number it increases gradually.

(ii) The slope increases with decreasing neutron number.

The second point is illustrated in fig. 4. For the lowest isotopes the $\alpha = \frac{1}{2}$ band is almost completely aligned (the maximal possible value for $i_{13/2}$ is $6.5\hbar$ for $\alpha = \frac{1}{2}$ and $5.5\hbar$ for $\alpha = -\frac{1}{2}$). For the heavier isotopes the aligned angular momentum decreases becoming $3.4\hbar$ and $2.7\hbar$, respectively, for the two signatures in $N = 99$. The agreement with the theoretical slopes of $E'_{\alpha\mu}(\omega)$ is surprisingly good. However the energetic signature splitting is systematically smaller for the theoretical quasiparticle levels (cf. also ^{167}Yb).

The trends of the slopes and the signature splitting reflect that the chemical potential, λ, shifts within the $i_{13/2}$ shell from the $\frac{7}{2}$ level ($N = 99$) to the $\frac{1}{2}$ level ($N = 89$). The odd neutron is relatively tightly bound to the deformed field in the middle of the $i_{13/2}$ shell whereas it is almost decoupled in the beginning of the shell.

6.3. TWO-QUASIPARTICLE EXCITATIONS IN AN EVEN-EVEN NUCLEUS

Example: ^{164}*Er*. Analysing an even-even nucleus one sees the two-quasiparticle excitations. The total signature may take the values $\alpha_t = 0, \pm 1$ and the angular

momentum is

$$I = 0, 2, 4, 6 \text{ etc. if } \alpha_t = 0, \text{ or}$$
$$I = 1, 3, 5, 7 \text{ etc. if } \alpha_t = \pm 1.$$

Fig. 5 shows the experimental Routhians of all bands identified in ^{164}Er [refs. [37-40])]. For comparison the energies of the relevant two-quasiparticle configurations as calculated from fig. 1 are also displayed. The g-band lies at $e' = 0$ because it serves as the reference.

The lowest two-quasiparticle configuration in fig. 1 is constructed by occupying the two neutron levels $[642\frac{5}{2}; \pm\frac{1}{2}]$ with positive energy (and freeing their conjugate partners). Its signature is $\alpha_t = 0$ and the parity $\pi = +$. We call it the s-configuration. Indeed the lowest two-quasiparticle band in experiment has $\alpha_t = 0$ and $\pi = +$ and we refer to it as the s-band (Stockholm- or super-band). As seen, the theoretical Routhian agrees well with the experimental one. The aligned angular momentum

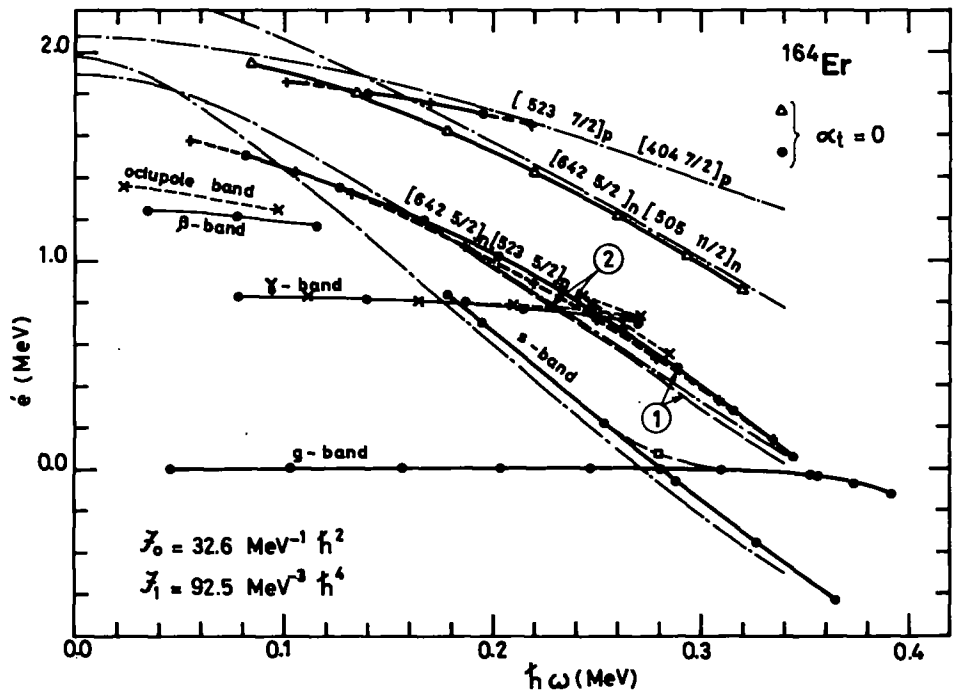

Fig. 5. Experimental Routhians for ^{164}Er. The solid lines and the marked out symbols indicate that the signature is $\alpha_t = 0$. The dashed lines and the remaining symbols indicate that $\alpha_t = 1$. The numbers 1 and 2 refer to the negative parity configurations discussed in the text. The value of K used in the analysis of the data is always the sum of the two Ω values indicated by the MO quantum numbers. The γ-band is evaluated with $K = 2$. For the g, s, β and octupole bands $K = 0$ is assumed. The thin long dashed and dashed dotted lines represent the calculated two-quasiparticle energies obtained as the sum of the corresponding one-quasiparticle energies in fig. 1.

of the s-band is about $8\hbar$ (cf. fig. 6b). This can be compared with the theoretical value $7.8\hbar$ obtained by adding the contributions from the theoretical levels $[642\frac{5}{2}; \pm\frac{1}{2}]$ and the value $7.9\hbar$ obtained from the experimental $[642\frac{5}{2}; \pm\frac{1}{2}]$ levels of ^{167}Yb.

At the frequency $\hbar\omega = 0.28$ MeV the g- and s-bands cross each other. This corresponds to the crossing of the levels $[642\frac{5}{2}; \pm\frac{1}{2}]$ in fig. 1 at $\hbar\omega = 0.036\hbar\omega_0 = 0.27$ MeV.

Fig. 6 shows the crossing of the g- and s-bands plotting the experimental lab

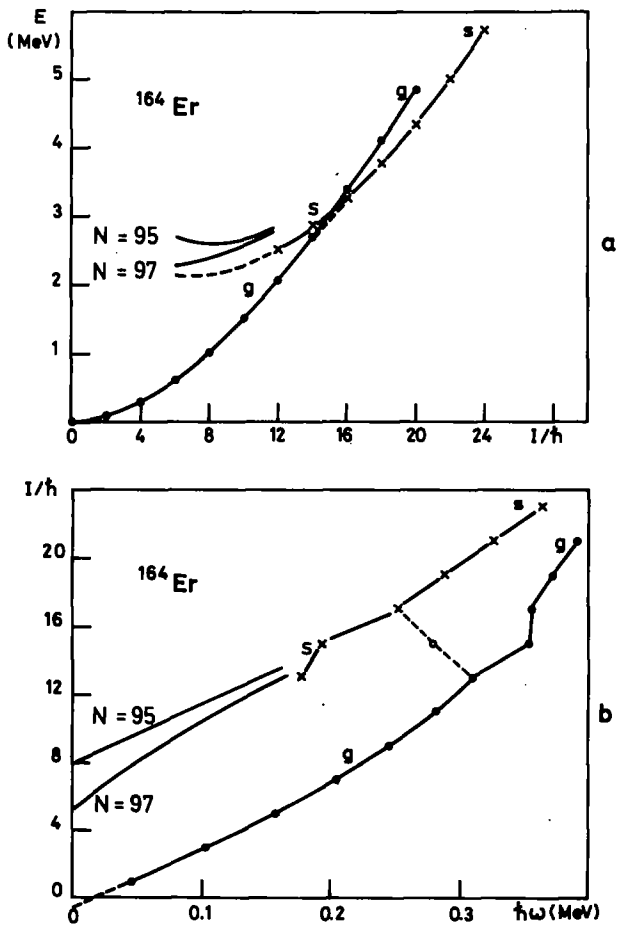

Fig. 6. The upper diagram shows the energies of the g-band and the s-band as functions of the angular momentum, while the lower diagram shows the angular momenta of the same bands as functions of the rotational frequency. The yrast line is described by the g-band for $I \leq 14\hbar$ and by the s-band for $I \geq 16\hbar$. By combining these two branches one obtains a backbending in the I versus $\hbar\omega$ diagram as indicated by the dashed line. The open circle represents the $16_s \rightarrow 14_s$ transition. The lines denoted by $N = 95, 97$ are predictions for the s-band calculated from the experimental Routhians in the corresponding odd mass Yb isotopes. The broken continuation of the s-band is obtained as their mean value, which has been shifted in order to meet the s-band.

energy E versus I. As indicated by the broken line the yrast sequence switches at $I = 16\hbar$ from the g- to the s-band. Fig. 6b displays the angular momentum I as a function of the frequency ω. Compared to the g-band the s-states additionally carry an almost constant amount of aligned angular momentum, which causes the backbending of the yrast sequence. The point on the broken line is calculated from the interband transition $16_s \rightarrow 14_g$. This corresponds in fig. 5 to the jump from the point at $\hbar\omega = 0.310$ MeV ($14_g^+ \rightarrow 12_g^+$) in the g-band to the point at $\hbar\omega = 0.253$ MeV ($18_s^+ \rightarrow 16_s^+$) in the s-band. The transition ($16_s^+ \rightarrow 14_g^+$) is indicated by the square at $\hbar\omega = 0.280$ MeV and $e' = 0.06$ MeV. We see that the sharp backbending in ^{164}Er arises simply from connecting two different bands to the yrast sequence. It should be mentioned that this interpretation of the backbending is equivalent with the alignment picture originally proposed by Stephens and Simon [41].

The s-band is observed down to the 12^+ state. It is not expected to terminate at this spin, because the one quasiparticle states $[642\frac{5}{2}; \pm\frac{1}{2}]$ it is built from have been observed in the adjacent odd neutron systems $N = 95$, 97 almost till $\omega = 0$ (cf. figs. 2, 3, 9). Considering the Routhians of these bands as "experimental quasiparticle levels" one can calculate i_s and e'_s of the s-band as the sum. Adding the known reference quantities I_g^x and E'_g one obtains $I_s(\omega)$, $E'_s(\omega)$ and by inverting the Legendre transformation (1.2) the lab energy $E_s(I)$ too. The corresponding predictions obtained from ^{165}Yb and ^{167}Yb are included in fig. 6. As seen, the predicted lower part of the s-band continues the trends of the observed part rather well. At $I = 6\hbar$ we reach $\omega \approx 0$. Within our frame it is not possible to say what will happen to the s-band at lower angular momentum. The level diagrams and figs. 2, 3 and 9 contain the necessary information to predict the lower part of the s-band in further nuclei.

The irregularities seen in fig. 6b at $I = 16\hbar$ can be attributed to a weak interaction of $V \approx 40$ keV between the crossing bands [38,40]. The theoretical counterpart is the interaction between the levels a, $-b$ and b, $-a$ at $\omega = 0.036\omega_0$ in fig. 1, which mixes the g- and the s-configuration. This mixture has a pathological character [42] because it acts at a given value of ω and mixes states with very different angular momentum. This leads at the crossing point to a strong dispersion of angular momentum, which is a signal that the theoretical description becomes questionable. Moreover, the way the s- and g-configurations interchange their characteristics leads to spurious branches in the theoretical functions $I(\omega)$ and $E(I)$. Similar conclusions have been drawn in refs. [16,43].

In ref. [42]) an elimination of the pathological mixture has been achieved by diagonalizing a particle-rotor like Hamiltonian within the two dimensional space spanned by the g- and s-configuration. As discussed above we use the simpler approach we suggested in ref. [20]). Assuming a constant interaction V between the two levels of equal signature we reconstruct the pure levels (thin lines in fig. 1) by means of eq. (4.1). These states define the pure s- and g-configurations. The interaction matrix element V between the s- and the g-configuration (half minimal level distance) is suggested to be equal to the interaction between the states of the g- and the s-band

having the same angular momentum I. Therefore, it should be compared with the experimental interaction. The value $V = 100$ keV calculated from fig. 1 agrees reasonably well with the experimental value of 40 keV (compared with the scale of V, cf. ref. [20])). Hence one may say, that the quasiparticle Routhian (2.1) provides a rather good description of the smooth behaviour of the levels. Near the crossings between levels of the same signature and parity the description becomes unreliable, because the mixture is described in the wrong way. Nevertheless, it contains the essential information about the crossing. More generally, if the levels show up a large curvature, their description by the quasiparticle Routhian is incorrect, like e.g. the $i_{\frac{13}{2}}$ levels near $\omega = 0$ in fig. 1. The pathological mixture between levels has no consequence if all of them are occupied because then it leaves the wave functions unchanged.

The crossing between the g- and the s-band is expected to be a general feature of the rare earth region (cf. subsect. 6.2). Whether this leads to a backbending in the yrast line or not depends on the magnitude of the interaction between the bands (for a quantitative criterion cf. ref. [20])). Due to a quantal interference the theoretical interaction matrix element shows an oscillating behaviour as a function of λ (cf. fig. 3), the origin of which has been explained in ref. [45]). In ref. [20]) we analysed the experimental data concerning the crossing of the g- and the s-bands in terms of a two-level model with constant interaction matrix element. The extracted quantities, i.e. crossing frequency, aligned angular momentum of the s-band and interaction matrix element, compare well with the corresponding theoretical values. The experimental interaction matrix element shows the oscillations predicted by theory. The nuclei with small interaction are sharp backbenders, whereas the ones with strong interaction show only a smooth upbending of $I_x(\omega)$ (or $\mathcal{J}_{\text{eff}}(\omega^2) = I_x(\omega)/\omega$). Similar results have been found in ref. [44]) by means of a model that couples $i_{\frac{13}{2}}$ particles to a rotor. The interaction matrix elements calculated there are about a factor of 2 larger than the values obtained from the quasiparticle levels. It is also stated that height of the peaks depends noticeably on the pairing strength Δ.

The characteristics of the s-band are only compatible with the assumption of strong pair correlations. Moreover, the very existence of both the g- and the s-band in the same nucleus is tied up to the existence of a pair field (see subsect. 6.8). The crossing of both bands is the manifestation of gapless superconductivity in the even system. The possibility of this phenomenon has been predicted in ref. [32]). Its relation to the backbending, has been first discussed in ref. [33]).

Before analysing the negative parity bands we should discuss the situation near the band heads. At low angular momenta one can ascribe to each band its total signature α_t and angular momentum projection K [cf. ref. [18]), ch. 5]. For one-quasiparticle excitations this classification coincides with the one of the quasiparticle levels in the low frequency limit. In the case of two-quasiparticle configurations there exist two combinations of the quasiparticle signatures $\alpha_1 + \alpha_2 = \alpha_t$ for given total signature α_t. They do not correspond to a good angular momentum projection $\hat{K}^2 = (\hat{K}_1 + \hat{K}_2)^2$. Their energies E' (rot. frame) differ only very little (if there is no

$K = \frac{1}{2}$ state involved). Thus a small perturbation that prefers good $\hat{K}^2$ may cause a transition to eigenstates of $\hat{K}^2$, where the symmetric and antisymmetric combinations correspond to the eigenvalues $(K_1 \pm K_2)^2$, respectively. The residual interaction between two quasiparticle states prefers states with good $\hat{K}^2$ (cf. below). Moreover, in the lab system at given I the energies of the two configurations $K = K_1 \pm K_2$ differ by the "zero point rotational energy" the difference having the order of $2K_1K_2/\mathcal{J}$ [cf. e.g. ref. [18]), eq. (4A-7)].

Therefore we ascribe each band the K given by I at the band head, which is then used in the analysis of the data (see subsect. 3). The parallel combination $K = K_1 + K_2$ lies below the antiparallel one and this explains why only such negative parity bands have been observed in ^{164}Er (cf. fig. 5). At high frequencies, where there is a sufficient spread in K_1 and K_2, the quasiparticle signatures α_1 and α_2 become good quantum numbers. Typically, this should occur when $E'(\omega = 0) - E'(\omega)$ (energy win due to K-mixing) is larger than $2K_1K_2/\mathcal{J}$ (splitting at the band head).

The lowest odd parity configurations that can be constructed are those involving the neutron levels $[642\frac{5}{2}]$ and $[523\frac{5}{2}]$. Considering the signatures we can distinguish between four different configurations, namely

(i) $[642\frac{5}{2}; \frac{1}{2}][523\frac{5}{2}; \frac{1}{2}]$ with $\alpha_t = 1$ (odd I),
(ii) $[642\frac{5}{2}; \frac{1}{2}][523\frac{5}{2}; -\frac{1}{2}]$ with $\alpha_t = 0$ (even I),
(iii) $[642\frac{5}{2}; -\frac{1}{2}][523\frac{5}{2}; \frac{1}{2}]$ with $\alpha_t = 0$ (even I),
(iv) $[642\frac{5}{2}; -\frac{1}{2}][523\frac{5}{2}; -\frac{1}{2}]$ with $\alpha_t = -1$ (odd I).

They are ordered so that the one with the lowest Routhian comes first. The difference in energy arises from the signature splitting (mainly due to $[642\frac{5}{2}]$).

When comparing with the experimental Routhians we find two close-lying bands with $\alpha_t = 0$ and 1, which start as a $K = 5$ $\Delta I = 1$ rotational sequence. The Routhians agree well with those constructed from the quasiparticle energy diagrams. At higher frequencies ($\hbar\omega > 0.2$ MeV), where we expect the quasiparticle signatures to become relevant, we propose to interpret the two bands as configurations (i) and (ii), because they are the lowest in energy. The Routhians of these configurations (if extended to somewhat higher frequencies) cross the g-band at $\hbar\omega = 0.35$ MeV. This crossing can be interpreted as the crossing of the $[642\frac{5}{2}; -\frac{1}{2}]$ level with the $[523\frac{5}{2}; \pm\frac{1}{2}]$ levels at $\hbar\omega = 0.046\ \hbar\omega_0 = 0.34$ MeV and the energy $0.055\ \hbar\omega_0$ in fig. 1. The configurations (i)–(iv) do not show backbending. The reason is the same as for ^{167}Yb. Both $[642\frac{5}{2}; \frac{1}{2}]$ levels are occupied. These features as well as the energy of the Routhians at the highest observed frequencies support the suggested interpretation of the two bands.

The two remaining configurations (iii) and (iv) have not been identified yet. Concerning their low frequency part one must take into account that the residual interaction mixes the quasiparticle configurations. An interaction of octupole-octupole type does not conserve the quasiparticle signatures preferring the $K = 0$ combination of the $[642\frac{5}{2}]$ and $[523\frac{5}{2}]$ levels. Indeed, this is the strongest neutron component in

the $K = 0^-$ octupole phonon state [46]). Only the lowest states of the octupole band are known experimentally, which are also shown in fig. 5. As seen, it lies noticeably below the two-quasiparticle bands $[642\frac{5}{2}][523\frac{5}{2}]$ but tends to meet them. The octupole interaction is expected to be less effective at higher frequency, because it prefers a large angle between the angular momenta of the two quasiparticles, whereas the Coriolis force tends to align them [47]). Therefore, the octupole band should develop into the missing configuration (iv). The actual nature of this transition remains an open question.

In experiment one sees a weak band with negative parity and signature zero, which starts at $I = 8$. This fact, the position of the Routhian and its slope, suggest the interpretation $[642\frac{5}{2}]_n[505\frac{11}{2}]_n$ $K = 8$.

One more signature pair of odd parity bands has been observed. Its properties differ from the bands containing the $[642\frac{5}{2}]_n$ level. The moment of inertia and the aligned angular momentum are smaller and it evidently has a band head at $I = 7\hbar$. A comparison with the quasiparticle energy diagrams (cf. fig. 8) suggests the assignment $[404\frac{7}{2}]_p[523\frac{7}{2}]_p$ i.e. the lowest two-quasiproton configuration, not showing any significant signature splitting. This assignment is supported by the β-decay of the ^{164}Tm ($I^\pi = 6^-$) isomer $[404\frac{7}{2}]_p[523\frac{5}{2}]_n$ which proceeds to the 1785 keV state of ^{164}Er. For the $[404\frac{7}{2}]_p[523\frac{7}{2}]_p$ states we can also distinguish between four different configurations depending on how we combine the signatures.

In the fig. 5 we have also included the β-band and the γ-band. The aligned angular momentum of the γ-band is almost zero as expected for a collective vibration. It shows backbending for both signatures at the same frequency as the yrast sequence. This could be connected with the crossing of the γ-vibration built on the s-band. It is also possible that the configurations $[642\frac{5}{2}\pm\frac{1}{2}]_n[633\frac{7}{2}\frac{1}{2}]_n$ cross the γ-band.

6.4. ONE- AND THREE-QUASIPARTICLE CONFIGURATIONS IN A NUCLEUS WITH ODD PROTON NUMBER

Example: ^{165}*Tm*. In fig. 7 we show the experimental Routhians for ^{165}Tm [ref. [48])]. At low frequencies the bands are of one-quasiparticle type and we therefore see the proton levels in fig. 7. On the whole, the theory reproduces the experimental results (relative position of the levels, slopes and signature splitting; compare figs. 7 and 8). However, the $[541\frac{1}{2}; \frac{1}{2}]$ level lies much too high compared to experiment whereas the slope is almost correct ($3.4\hbar$ compared to the experimental value $3.2\hbar$). It is possible that an excitation to the $[541\frac{1}{2}; \frac{1}{2}]$ level, which is strongly deformation driving, might introduce an increase of the deformation. It is in fact possible to get the level down to the right position by increasing ε_2 from 0.26 to 0.30.

As in the neutron system, there are also proton levels entering the gap region with a steep slope. Thus, gapless superconductivity is present in the proton system too. The states $[523\frac{7}{2}; \pm\frac{1}{2}]$ belong to the $h_{\frac{11}{2}}$ multiplet that plays an analogous role as $i_{\frac{13}{2}}$ in the neutron case. However, in addition there is the $[541\frac{1}{2}; \frac{1}{2}]$ level, which descends very rapidly, becoming the state with the lowest experimental Routhian.

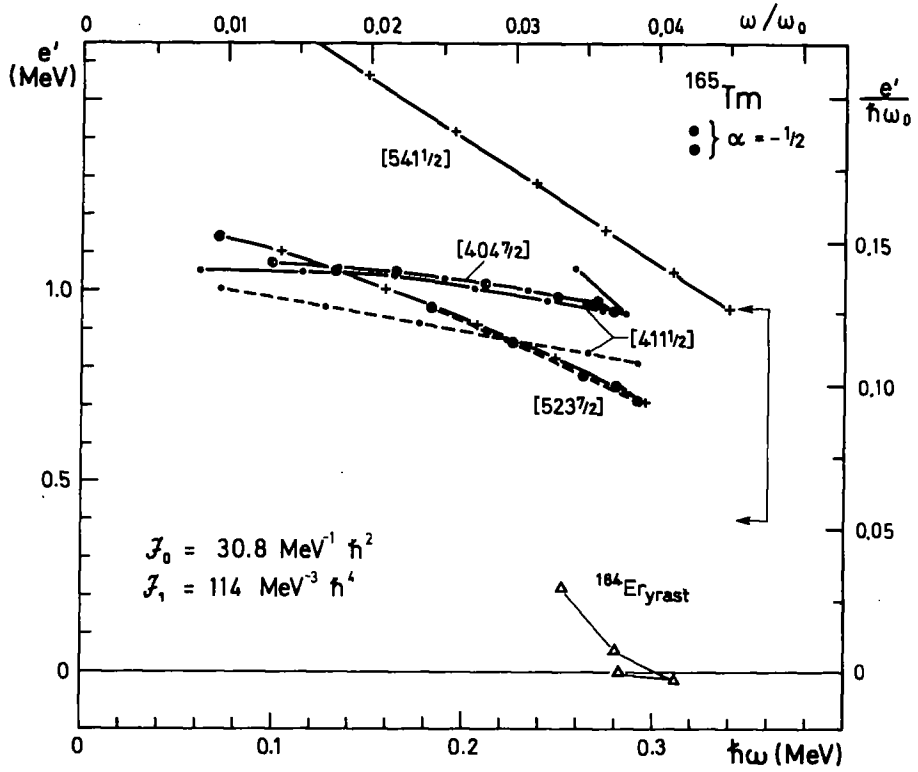

Fig. 7. Experimental Routhians for ^{165}Tm. For comparison, we have also included the Routhian, which corresponds to the yrast sequence of ^{164}Er. The Routhian of the $[541\ \frac{1}{2}; \frac{1}{2}]$ band is shifted to higher energies.

At $\hbar\omega \approx 0.28$ MeV we find that the bands $[404\frac{7}{2}; \pm\frac{1}{2}]$, $[411\frac{1}{2}; \frac{1}{2}]$ and $[523\frac{7}{2}; -\frac{1}{2}]$ backbend. This must be understood as a neutron effect, i.e. the neutrons change from the g- to the s-configuration. Consequently, the backbending frequency agrees with the one of ^{164}Er, which has the same neutron system as ^{165}Tm. The Routhian of the yrast sequence of ^{164}Er is also shown in fig. 7 (cf. the discussion of ^{164}Er).

The $[541\frac{1}{2}; \frac{1}{2}]$ band continues through the backbending region without showing any irregularity. In fact a different deformation of this configuration may cause the disappearance of backbending. This has been demonstrated in ref. [24]) for the isotone ^{167}Lu, which also does not show backbending in the $[541\frac{1}{2}; \frac{1}{2}]$ band [49]). A calculation with the increased deformation $\varepsilon_2 = 0.29$ (about the increase calculated in ref. [24])) shows that the $N = 98$ bumb of the interaction matrix element (cf. fig. 4 of ref. [20])) becomes wider, such that both $N = 96$ and 98 are near the interaction maximum. This may explain the absence of backbending in the $[541\frac{1}{2}; \frac{1}{2}]$ bands of ^{165}Tm, ^{167}Lu and ^{169}Lu [ref. [50])]. However, according to this calculation ^{163}Tm should show

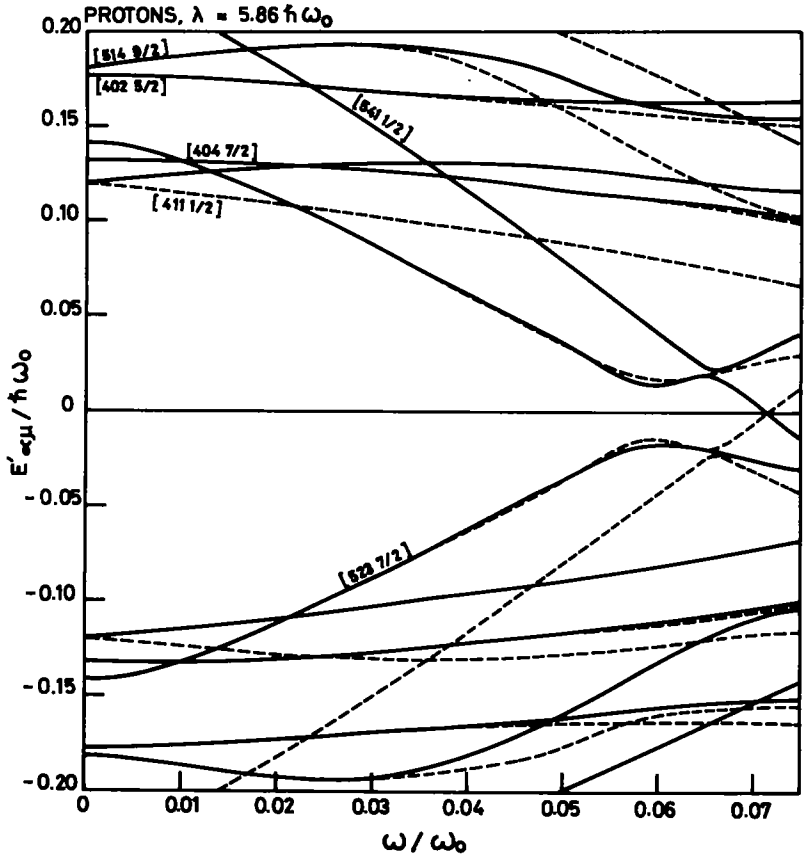

Fig. 8. Quasiparticle energy diagram, calculated for $\lambda = 5.86\hbar\omega_0$, corresponding approximatively to proton number Z = 69.

backbending in contradiction to the experiment [51]). We feel that a more careful investigation of this problem is necessary before one can draw definitive conclusions.

6.5. ONE- AND THREE-QUASIPARTICLE CONFIGURATIONS IN NUCLEI WITH ODD NEUTRON NUMBER

Examples: $^{163,165}Yb$. The experimental Routhians [52]) of ^{163,165}Yb are shown in fig. 9. They should be compared with the quasiparticle levels in fig. 10, which corresponds to $N \approx 94$.

The experimental $[523\frac{5}{2}; \frac{1}{2}]$ band shows a clear backbending at $\hbar\omega \approx 0.24$ MeV in both isotopes. The odd particle is in an odd parity level and does not interfere with the even parity levels responsible for the backbending. The frequency is somewhat smaller than for the nearlying even Yb isotopes ($\hbar\omega \approx 0.27$ MeV). Beyond the

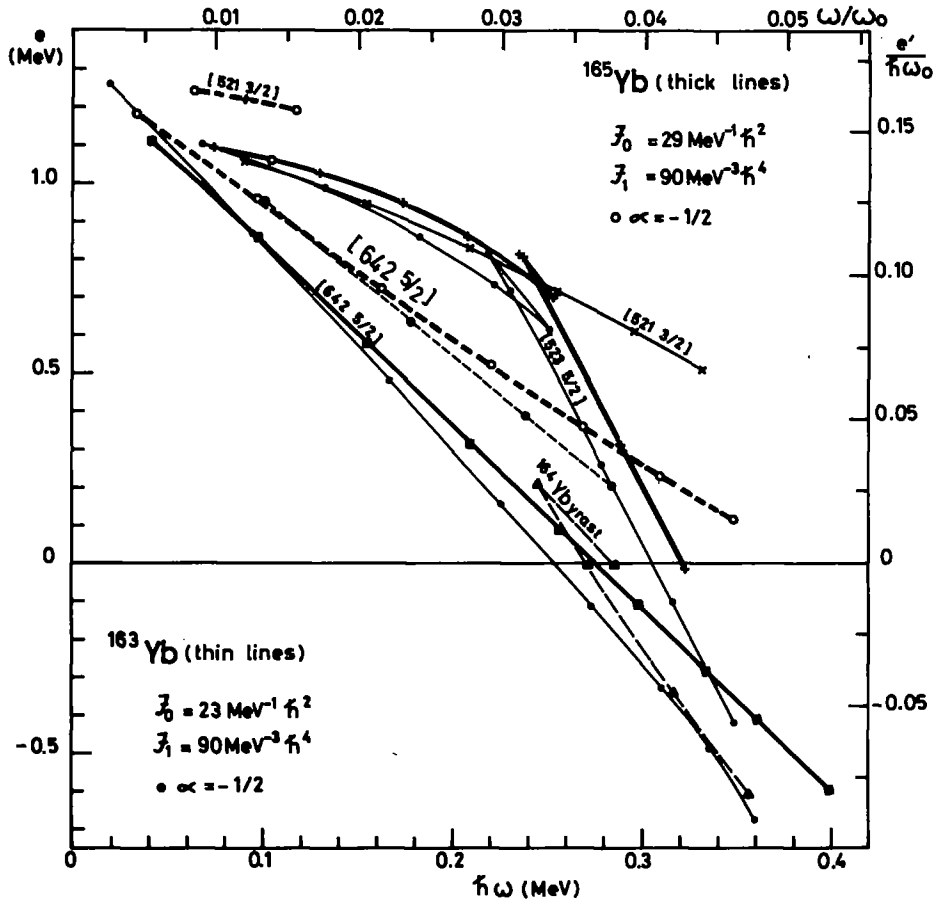

Fig. 9. The experimental Routhians for ^{163}Yb (thin lines) and ^{165}Yb (thick lines). For comparison the yrast sequence of ^{164}Yb (cf. ref. [11])) is also displayed.

backbending region the $[523\frac{5}{2}; \frac{1}{2}]$ band has an aligned angular momentum of 9.2$\hbar$ and 9.5$\hbar$, respectively, for ^{165}Yb and ^{163}Yb. This should be compared with the sum of the aligned angular momentum of the $[523\frac{5}{2}; \frac{1}{2}]$ band before the backbending, which is 2.7$\hbar$ and 2.5$\hbar$ respectively, and the aligned angular momentum of the s-band in the adjacent even Yb isotopes (7.8$\hbar$ in ^{166}Yb and 7.7$\hbar$ in ^{164}Yb), as well as with the values calculated from fig. 10, which are 1.8$\hbar$ for $[523\frac{5}{2}; \frac{1}{2}]$ and 9$\hbar$ for $[523\frac{5}{2}; \frac{1}{2}]$ $[642\frac{5}{2}; -\frac{1}{2}]$ $[642\frac{5}{2}; \frac{1}{2}]$. The aligned angular momentum supports the interpretation of the $[523\frac{5}{2}; \frac{1}{2}]$ band after the backbending as a one quasiparticle excitation built on the s-band.

In ^{163}Yb the Routhian of the $[521\frac{3}{2}; \frac{1}{2}]$ band has been observed beyond the backbending region without showing any irregularities, although it is expected to back-

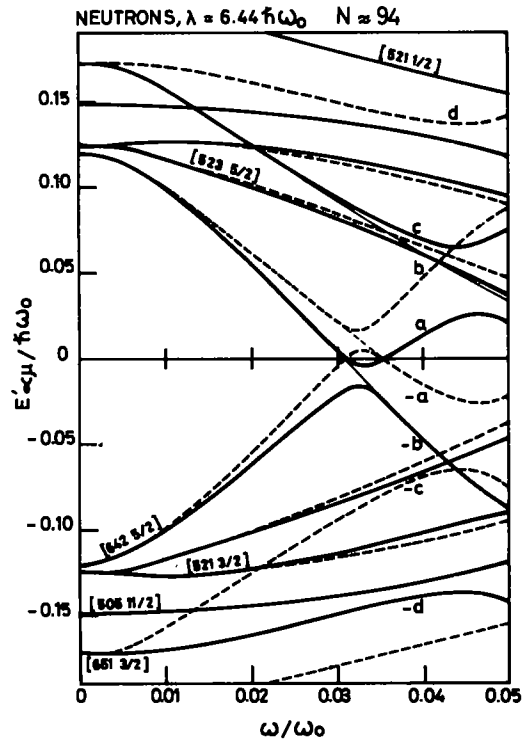

Fig. 10. Quasiparticle energy diagram, calculated for $\lambda = 6.44\hbar\omega_0$, corresponding approximatively to neutron number $N = 94$.

bend as well. The reason remains an open question. A more systematic experimental study of this effect (especially its dependence on proton and neutron number) would be very helpful for clarification.

6.6. HIGHER CROSSINGS IN THE $i_{13/2}$ SHELL

So far we have only considered the first level crossing within the $i_{\frac{13}{2}}$ shell. Taking fig. 10 as an example, it lies at $\omega = 0.033\omega_0$. The second crossing occurs between the levels a and c at $\omega = 0.045\omega_0$. It is expected to show up as an irregularity of the lowest $i_{\frac{13}{2}}\,\alpha = \frac{1}{2}$ band in odd neutron nuclei, because in this configuration the level a is occupied but c is free. One may say that, in addition to the odd neutron, two further $i_{\frac{13}{2}}$ neutrons align their angular momentum. According to figs. 3 and 10 the resulting three-quasiparticle state is expected to carry about $13\hbar$ aligned angular momentum.

Fig. 11 shows that the interaction at the second crossing is also an oscillating function of the neutron number, as pointed out in ref. [45]). The oscillations are not in phase with those of the first crossing (compare fig. 4, ref. [20])). Similar interaction functions have been obtained in ref. [44]) on the basis of a particle-rotor model.

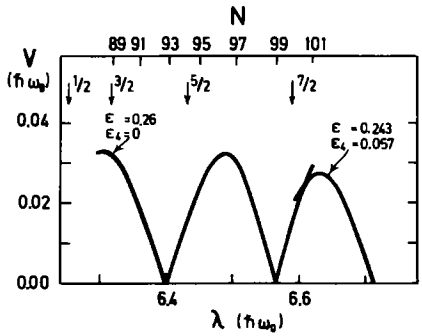

Fig. 11. The interaction matrix element V for the second crossing of the $i_{13/2}$ levels as a function of neutron number. Note for large values of N a deformation different from the standard values in this publication is used.

In the nuclides ^{159,161}Yb [ref. [53])], $^{163-167}$Yb and ^{157,159}Er the lowest $i_{13/2}$ $\alpha = \frac{1}{2}$ band is measured up to frequencies where we expect the second crossing. The aligned angular momentum $i(\omega)$ of these bands is shown in fig. 12. In the case of the neutron numbers $N = 91, 93$ there is a significant upbending visible. The frequency $\hbar\omega \approx 0.35$ MeV agrees well with the location of the crossing a, c in fig. 10 ($\hbar\omega = 0.34$ MeV). The absence of the rapid upbending for $N = 89$ and 95 may be understood from the interaction pattern in fig. 11. A sharp crossing is expected for $N = 93$ and 99. If one allows for some uncertainty in the particle number, one may suggest that $N = 93$ and 91 lie approximately symmetric to the zero point at $\lambda = 6.4\hbar\omega_0$. Accordingly they show a rapid upbending. The neutron number $N = 89$ and 95 should then

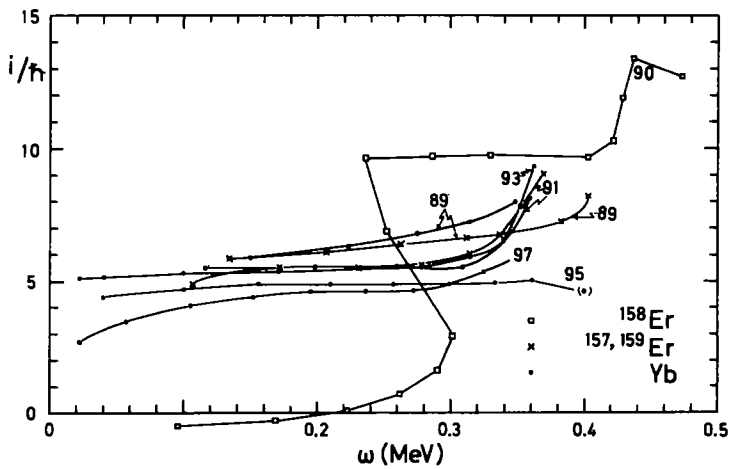

Fig. 12. The experimental aligned angular momentum i as function of ω for $N = 89$–97 nuclides and ^{158}Er. The parameters of the analysis are ^{158}Er: $\mathcal{J}_0 = 20$ MeV$^{-1}\cdot\hbar^2$ $\mathcal{J}_1 = 90$ MeV$^{-3}\cdot\hbar^4$ $K = 0$, ^{159}Yb: $\mathcal{J}_0 = 12$ MeV$^{-1}\cdot\hbar^2$ $\mathcal{J}_1 = 90$ MeV$^{-3}\cdot\hbar^4$ $K = \frac{1}{2}$, ^{161}Yb: $\mathcal{J}_0 = 19$ MeV$^{-1}\cdot\hbar^2$ $\mathcal{J}_1 = 90$ MeV$^{-3}\cdot\hbar^4$ $K = \frac{1}{2}$. The parameters of the odd mass Er isotopes are given in fig. 3.

be located near interaction maxima and thus behave more smoothly. The fact that the upbending appears in both the Yb and Er isotopes for the neutron number 91 strongly supports the interpretation as a neutron effect.

Slightly above the second crossing (*ac*) we find the third crossing (*bd*) at $\omega \approx 0.048\omega_0$. It should cause an irregularity in the lowest $i_{13/2}$ $\alpha = -\frac{1}{2}$ one-quasiparticle band.

Both crossings, just discussed, appear in the g-configuration (*a*, *b* occupied) of the even system. Therefore, after the crossing with the s-band, the g-band should meet two further bands with a large aligned angular momentum. The s-configuration does not reveal the crossings, because the interacting levels are either both occupied or both free. This is in accordance with the experimental data [54]) on ^{158}Er, also shown in fig. 12. After the g-s crossing at $\hbar\omega \approx 0.26$ MeV the yrast line follows the s-band, which does not show any irregularity up to $\hbar\omega = 0.40$ MeV.

6.7. BACKBENDING IN THE PROTON SYSTEM

The $h_{11/2}$ levels of the proton system behave similarly to the $i_{13/2}$ neutron states (see fig. 8). One can construct a proton s-configuration from the two lowest signatures. In fig. 8, corresponding to $Z \approx 69$, these are the levels $[523\frac{7}{2}; \pm\frac{1}{2}]$. The crossing between the s- and the g-configuration lies at $\omega = 0.059\omega_0$. Fig. 13 shows the interaction matrix element as a function of the proton number Z. As seen, sharp backbending is expected for the zero points of V near $Z = 62$, 68 and 76.

The yrast levels of the isotones ^{156}Dy (ref. [55])), ^{158}Er (ref. [54])) and ^{160}Yb (ref. [56])) have been measured up to frequencies where the proton g- and s-configurations are expected to cross. We interpret the second irregularity of the function $i(\omega)$ for ^{158}Er as this crossing (see fig. 12). The experimental frequency $\hbar\omega = 0.43$ MeV and the aligned angular momentum $4\hbar$ are to be compared with the values 0.45 MeV and $6\hbar$ calculated from fig. 8.

The crossing is also seen in ^{160}Yb whose function $i(\omega)$ is very similar to the one of ^{158}Er. However ^{156}Dy behaves regularly at the crossing frequency. This pattern fits

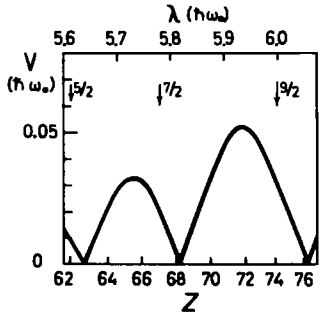

Fig. 13. The interaction matrix element V for the first crossing of the $h_{11/2}$ levels as a function of proton number.

qualitatively with the behaviour of the interaction shown in fig. 13 if one allows for a slight shift of the zero from $Z = 68$ to $Z \approx 69$. Such a shift can be understood if one recognizes that the deformation of these nuclei is $\varepsilon \approx 0.20$ and $\varepsilon_4 \approx -0.02$. Compared to the deformation $\varepsilon = 0.26$ and $\varepsilon_4 = 0.00$, used in fig. 13, the single-particle levels $[404\frac{7}{2}]$ and $[402\frac{5}{2}]$ come down to the vicinity of the Fermi surface. As a consequence the Fermi level is lowered relative to the $h_{\frac{11}{2}}$ levels, especially for ^{160}Yb but partially also for ^{158}Er, causing a shift of the interaction minimum to around $Z = 69$.

6.8. THE QUASIPARTICLE ENERGIES AT VERY HIGH FREQUENCIES

We have extended two of the diagrams (figs. 1 and 8) to illustrate what can be expected to happen at frequencies above $0.05\omega_0$. In this region we expect Δ to decrease towards zero. Changes of the deformation should also occur, as shown by calculations without pairing [1,6,8]). In fig. 1 we have taken into account changes in Δ in a schematic way, by assuming a linear decrease from the full value $0.12\hbar\omega_0$ at $\omega = 0.05\omega_0$ to zero at $\omega = 0.10\omega_0$.

At high frequencies the g-configuration looses its identity. It is then better to refer to the vacuum because it represents yrast states. As already said, the vacuum is defined as the lowest configuration with *even* particle number. This is essential at the crossing of the levels a and $-a$ above which $[-a]$ becomes vacuum (concerning the labelling, cf. the beginning of sect. 6). Above the crossing between the levels a and $-c$ the vacuum is $[c]$ having $\pi = -$ and $\alpha_t = 1$. This state is the continuation of the negative parity configuration denoted by (i) in subsect. 6.3. Provided that the quasiparticle levels are sufficiently realistic, it would be expected to become yrast for $\hbar\omega \gtrsim 0.44$ MeV.

At $\omega = 0.10\omega_0$, Δ is equal to zero and therefore one-half of the quasiparticle levels coincide with the eigenvalues $\varepsilon'_{\alpha l}$ of the single-particle Routhian, $h'_{\text{s.p.}}$. These levels are shown to the right in fig. 1 as thick lines. By reflecting them in the Fermi surface we get the other half of the quasiparticle levels, displayed as thin lines. Thus for $\Delta = 0$ the quasiparticle levels can be classified as either pure "particle states", corresponding to the eigenstates of $h'_{\text{s.p.}}$, or pure "hole states".

At $\omega = 0.10\omega_0$ the vacuum becomes identical to the single-particle configuration with all levels up to $[523\frac{5}{2}; \frac{1}{2}]$ occupied. A part of the excited quasiparticle configurations becomes particle-hole excitations, like e.g. $[-c, d]$. However, other excitations lead to a different particle number, like e.g. $[-a, d]$ that corresponds to the lowest $N = 98$ state. Hence, the pair correlations enable additional excitations, that would correspond to a different particle number in the unpaired system. An example of this kind is the s-configuration. The very existence of the g- and the s-configuration in one and the same nucleus is only possible if there are substantiel pair correlations.

7. Conclusions

We demonstrated that it is possible to construct the (non-collective) spectra in the yrast region of deformed rotating nuclei from basic units, the quasiparticle levels. The decisive step in achieving this is to consider the angular frequency and the energy in the rotating frame (Routhian) instead of the angular momentum and the lab. energy, which are the immediate experimental results. This transformation invokes additivity, i.e. at given ω the Routhian of e.g. a two-quasiparticle excitation is just the sum of the Routhians of the two relevant one quasiparticle states. This means we extended the familiar analysis of low-lying states in terms of quasiparticle levels to the lower part of the yrast region ($I \lesssim 30\hbar$). The combination of quasiparticle levels to one, two, three, ... quasiparticle configurations generates the whole variety of yrast spectra observed in experiment. Thus, the theoretical quasiparticle energy diagrams are very condensed pieces of information for a survey of the yrast spectrum. They are relatively easy to calculate, since the computational effort is significantly lower than for self-consistent calculations.

When analysing the experimental data it is important that the rotational states are classified with respect to the parity and the signature. The slope of the experimental Routhian, i.e. the aligned angular momentum, provides additional information for the identification of the different quasiparticle configurations, especially in cases where high angular momenta are involved.

The experimental Routhian, combined with the quasiparticle energy diagrams, is the key for systemizing the experimental information about the yrast spectra, but even without using the theoretical diagrams one can establish useful relations between data, because the measurements of the odd-mass spectra provide "experimental quasiparticle energy diagrams".

An essential point for understanding the backbending phenomenon is the fact that it is controlled by the magnitude of the interaction between the crossing bands, which is an oscillating function of particle number. The correlation between the particle number and interaction strength permits a deeper insight into the backbending mechanism. It may serve to distinguish between protons and neutrons or between different kinds of band crossings.

Analysing the various examples of experimental spectra, we stated several predictions explicitly. However, the level diagrams contain a vast amount of information about two-, three-, ... quasiparticle bands that may be checked experimentally.

The theoretical diagrams calculated with the constant quadrupole deformation $\varepsilon_2 = 0.26$ and the gap fixed to about the ground state value rather well account for the observed yrast spectra. Thus, this choice of parameters should be reasonable in the considered region. Especially the strong alignment of the odd neutron $i_{13/2}$ bands and the existence of the s-band are rather compelling evidence for a finite (and large) value of Δ up to an angular momentum of about $20\hbar$. This seems to indicate the necessity for more sophisticated treatments of the pair field than the usual Hartree-Fock-Boguljubov theory in order to understand the magnitude of Δ.

There are, however, a number of questions which deserve a closer investigation:

(i) The slopes of the quasiparticle levels, which are reproduced very well in our model, and their relation to the attenuation problem faced in the particle-rotor model.

(ii) The consequences of angular momentum conservation. Especially, the intuitive way we treat the crossing of bands with a finite interaction should be put on a more solid theoretical basis.

(iii) The influence of changes of the deformation and the pair field as functions of ω, the particle number and the configuration.

(iv) The possibility and the consequences of new components in the average field and the pair field due to the breaking of the time reversal symmetry.

We want to express our gratitude to A. Bohr and B. Mottelson for drawing our attention to the importance of the quasiparticle level diagrams, and for many helpful discussions and valuable suggestions. We are also grateful to T. Døssing, I. Hamamoto, E. R. Marshalek, K. Matsuyanagi, L. Münchow and K. Neergård for numerous discussions. S.F. thanks the Danish Ministry of Education for a grant.

References

1) K. Neergard, V. V. Pashkevich and S. Frauendorf, Nucl. Phys. **A262** (1976) 61
2) B. Banerjee, H. J. Mang and P. Ring, Nucl. Phys. **A215** (1973) 366
3) P. C. Bhargava and D. J. Thouless, Nucl. Phys. **A215** (1973) 515
4) A. Faessler, K. R. Sandhya Devi, F. Grümmer, K. W. Schmid and R. R. Hilton, Nucl. Phys. **A256** (1976) 106
5) A. L. Goodman, Nucl. Phys. **A265** (1976) 113
6) G. Andersson, S. E. Larsson, G. Leander, P. Möller, S. G. Nilsson, I. Ragnarsson, S. Åberg, R. Bengtsson, J. Dudek, B. Nerlo-Pomorska, K. Pomorski and Z. Szymański, Nucl. Phys. **A268** (1976) 205
7) M. Ploszajczak, K. R. Sandhya Devi and A. Faessler, Z. Phys. **A282** (1977) 267
8) K. Neergård, H. Toki, M. Ploszajczak and A. Faessler, Nucl. Phys. **A287** (1977) 48
9) R. A. Sorensen, Rev. Mod. Phys. **45** (1973) 353
10) F. S. Stephens, Rev. Mod. Phys. **47** (1975) 43
11) R. M. Lieder and H. Ryde, in Advances in nuclear physics, ed. E. Vogt and M. Baranger, vol. 10 (Plenum, NY, 1977)
12) A. Bohr and B. Mottelson, Proc. Int. Conf. nuclear structure, Tokyo, Sept. 5–10, 1977, J. Phys. Soc. Japan **44** (1978), suppl. p. 157
13) H. J. Mang, Phys. Reports **18C** (1975) 327
14) A. L. Goodman, Nucl. Phys. **A230** (1974) 466
15) S. G. Nilsson, C. F. Tsang, A. Sobiczewski, Z. Szymański, S. Wycech, G. Gustafsson, I. L. Lamm, P. Möller and B. Nilsson, Nucl. Phys. **A131** (1969) 1
16) E. R. Marshalek and A. L. Goodman, Nucl. Phys. **A294** (1978) 92;
E. R. Marshalek, private communication
17) J. G. Valatin, Phys. Rev. **122** (1961) 1012
18) A. Bohr and B. Mottelson, Nuclear structure, vols. I and II (Benjamin, New York, 1969 and 1975)
19) R. Beck, H. J. Mang and P. Ring, Z. Phys. **231** (1970) 26
20) R. Bengtsson and S. Frauendorf, preprint NORDITA-78/19; Nucl. Phys. **A314** (1979) 27
21) S. M. Harris, Phys. Rev. **138** (1965) B509
22) M. A. J. Mariocotti, G. Scharff-Goldhaber and B. Buck, Phys. Rev. **178** (1969) 1864
23) C. W. Ma and C. F. Tsang, Phys. Rev. **C11** (1970) 798 and earlier work quoted therein
24) A. Faessler, K. R. Sandhya Devi and A. Barroso, Nucl. Phys. **A286** (1977) 101

25) S. Frauendorf, Nucl. Phys. **A263** (1976) 150
26) R. Bengtsson and S. Frauendorf, Proc. Int. Symp. on high-spin states and nuclear structure, Dresden 1977, p. 74
27) Th. Lindblad, Nucl. Phys. **A238** (1975) 287
28) B. J. Meijer, F. W. N. de Boer and P. F. A. Goudsmit, Nucl. Phys. **A259** (1976) 213
29) I. O. Meredith and R. C. Barber, Can. J. Phys. **50** (1972) 1195
30) A. H. Wapstra and N. B. Grove, Nucl. Data Tables **9** (1971) 265
31) A. Abrikosov and L. Gorkov, JETP (Sov. Phys.) **12** (1961) 1243
32) A. Goswami, L. Lin and G. L. Struble, Phys. Rev. Lett. **25B** (1967) 451
33) Yu. T. Grin, Phys. Lett. **52B** (1974) 135
34) E. Grosse, F. S. Stephens and R. M. Diamond, Phys. Rev. Lett. **31** (1973) 840
35) S. A. Hjorth, H. Ryde, K. A. Hagemann, G. Løvhøjden and J. C. Waddington, Nucl. Phys. **A144** (1970) 513
36) E. Selin, S. A. Hjorth and H. Ryde, Physica Scripta **2** (1970) 181
37) O. C. Kistner, A. W. Sunyar and E. Mateosian, Phys. Rev. **C17** (1978) 1417
38) N. R. Johnson, S. W. Yates, L. L. Riedinger, A. C. Kahler, R. M. Ronningen and R. D. Hichwa, Proc. Int. Conf. on nuclear structure, Tokyo, 1977, Vol. I, p. 409.
39) A. Bayrn, Nucl. Data Sheets **11** (1974) 327
40) I. Y. Lee, D. Cline, R. S. Simon, P. A. Butler, P. Colombani, M. W. Guidry, F. S. Stephens, R. M. Diamond, N. R. Johnson and E. Eichler, Phys. Rev. Lett. **17** (1976) 420
41) F. S. Stephens and R. S. Simon, Nucl. Phys. **A183** (1972) 257
42) I. Hamamoto, Nucl. Phys. **A271** (1976) 15
43) F. Gruemmer, K. W. Schmid and A. Faessler, Nucl. Phys. **A306** (1978) 134
44) J. Almberger, I. Hamamoto and G. Leander, Phys. Lett. **80B** (1979) 153
45) R. Bengtsson, I. Hamamoto and B. Mottelson, Phys. Lett. **73B** (1978) 259
46) K. Neergård, private communication
47) P. Vogel, Phys. Lett. **60B** (1976) 431
48) C. Foin, S. Andre and D. Barneoud, Phys. Rev. Lett. **35** (1975) 1697
49) C. Foin and D. Barneoud, Phys. Rev. Lett. **33** (1974) 1049
50) C. Foin, D. Barneoud, S. A. Hjorth and R. Bethoux, Nucl. Phys. **A199** (1973) 129
51) C. Foin, S. Andre and D. Barneoud, Nucl. Phys. **A289** (1977) 77
52) L. Richter, H. Backe, E. Kankeleit, F. Weik and R. Willwater, Phys Lett. **71B** (1977) 74
53) O. J. Donahue, O. Häusser, R. L. Hershberger, K. E. G. Löbner, R. Lutter, O. Proetel and F. Riess, Beschleunigerlaboratorium der Universität und Technischen Universität München Annual report 1975, pp. 76, 78
54) I. Y. Lee, M. M. Aleonard, M. A. Deleplanque, Y. El-Masri, J. O. Newton, R. S. Simon, R. M. Diamond and F. S. Stephens, Phys. Rev. Lett. **38** (1977) 1454
55) D. Ward, O. Hausser, H. R. Andrews, B. Haas, P. Skensved and M. Maynard, Int. Conf. on nuclear interactions, Canberra, 1978
56) F. A. Beck, E. Bożek, T. Byrski, C. Gehringer, J. C. Merdinger, Y. Schutz. J. Styczen and J. P. Vivien, Phys. Rev. Lett. **42** (1979) 493
57) A. Faessler and M. Ploszajczak, Phys. Lett. **76B** (1978) 1